NASA CONTRACTOR
REPORT

NASA CR-11

NASA CR-1186

FLOW-INDUCED VIBRATIONS OF A FLAT PLATE SUSPENDED IN A NARROW CHANNEL

by Franklin T. Dodge and Arthur F. Muller

NATIONAL AERONAUTICS AND SPACE ADMINISTRATION • WASHINGTON, D. C. • SEPTEMBER 1968

Sep 68

FLOW-INDUCED VIBRATIONS OF A FLAT PLATE

SUSPENDED IN A NARROW CHANNEL, final report.

By Franklin T. Dodge and Arthur F. Muller

TABLE OF CONTENTS

FLOW-INDUCED VIBRATIONS OF A FLAT PLATE

SUSPENDED IN A NARROW CHANNEL

By Franklin T. Dodge and Arthur F. Muller
Southwest Research Institute

SUMMARY

Elastically restrained plates in narrow flow channels can vibrate
excessively when the flow rate past them reaches some critical value.
Because of the importance of this phenomenon in nuclear reactor design,
an analytical study of such vibrations has been conducted. The theory
is based upon the one-dimensional, hydraulic flow assumption and includes
viscous pressure drops and energy losses at channel contractions and
expansions. Since the vibrating plate influences the hydrodynamic load-
ing and vice versa, the unknown flow velocity and plate vibration frequency
are coupled and must be determined simultaneously. The results of the
calculations for several typical flow situations show that the flow velocity
necessary to induce vibrations decreases as the channel height-to-plate
length ratio decreases; this is in substantial agreement with previous
potential flow calculations although not with experimental data.

INTRODUCTION

Many challenging problems have been encountered during the hydraulic
and thermal parts of the design of nuclear reactors. For example, special
"no-leak" high pressure pumps had to be built to prevent radioactive con-
tamination through leakage of the coolant flow. In other cases, new analyses
or concepts had to be developed. For example, the idea of a "hot channel
factor" has been devised to establish the maximum permissible heat flux in
the core. Likewise, magnetohydrodynamic pumps first came into use for
pumping the liquid metal coolant used in some reactors.

The fluid flowing by the fuel elements and control rods is a source
of much design concern. Fuel elements and control rods are contained in
what are essentially narrow channels, and the flow of fluid down these nar-
row channels must be sufficiently high to keep the temperature within safe
limits. Small changes in the flow rate or the channel clearances result in
rather large changes in the heat released so both the flow rate and the
channel dimensions must be carefully controlled. In order to keep the core
small and the energy release high, it is desirable to have large flow rates;

but, aeronautical history has demonstrated that high-speed flow along an elastic structure can sometimes lead to disastrous self-excited vibrations of the structure. Indeed, it has also been observed that in nuclear reactors, the control rods or the fuel elements, or both, can vibrate excessively when the flow reaches some critical value. These kinds of vibrations seem to have been the cause of the failure of the core of the Kiwi B-4A nuclear rocket engine (ref. 1); flow induced vibrations also were evident in certain components of the Rowe Power Plant of the Yankee Atomic Electric Company (ref. 2).

Even though the problems with the Kiwi engine and other reactors have been corrected by a series of mechanical "fixes," important reasons still exist for obtaining a better understanding of the physical mechanisms causing the vibrations. Narrow channel flow, which came into prominence in pressurized water reactors, is becoming more common in high density heat exchangers, so the ability to predict flow-induced vibrations ahead of time and then make necessary changes in the design will be of considerable value. For this reason, some previous research has already been conducted. Burgreen, et al. (ref. 3) made an experimental study of several typical heat-exchanger tube bundles and found, apparently, that vibrations of the rods could be excited over a wide range of flow velocities past them. From these studies, they concluded that the vibrations were self-excited and not a result of the shedding of von Karman vortices. Bland, et al. (ref. 4), of NASA-Langley conducted a combined experimental and theoretical study of a rigid plate elastically suspended in a two-dimensional flow channel. Their analysis predicted the onset of vibrations fairly well for wide channels but did not agree with experimental results for narrower ones. Miller and Kennison (ref. 2) of Knolls Atomic Power Laboratory made a hydraulic-flow analysis of the vibrations of a rigid plate in a narrow channel. Although their results did not agree with their experimental tests, they did show that there were some positions of the plate in the channel that were more stable than others.

The purpose of the analysis presented in this report, which was undertaken in conjunction with the experimental program conducted by NASA mentioned previously (ref. 4), was to discover if a simplified hydraulic flow approximation would or would not be sufficient to explain the variation of the critical flow velocity with channel height for narrow channels. Thus, the analysis is complementary to the potential flow theory given in ref. 4, which applies to wide channels.

SYMBOLS

a thickness of plate

A b/H, ratio of plate length to channel height

b	length of plate
C_h	damping coefficient for translational plate motions
C_α	damping coefficent for pitching plate motions

$\mathscr{D} = HW \left[\dfrac{H}{2} + \sigma(W - W_s) \right]^{-1}$, hydraulic diameter of channels

F	friction factor for channels A or B when plate is centered in the main channel

$\mathscr{F} = Fb/\nu$, frictional pressure drop factor

h	displacement of leading edge of plate from centerline of channel
$h_{e.a.}$	displacement of translation spring at elastic axis
H	height of main channel
I_α	mass moment of inertia about the elastic axis, per unit width of plate
K_D	loss coefficient for cross-flow mixing around sides of plate
K_h	spring constant of translation spring
K_L	loss coefficient at leading edge of plate

$K_{Lh} = \dfrac{dK_L}{dh}$, rate of change of K_L with translation of plate

K_α	spring constant of pitch spring

$K_{L\alpha} = \dfrac{1}{2} b \dfrac{dK_L}{dh}$, rate of change of K_L with pitching of plate

m	total translating mass per unit plate width
N_{Re}	Reynolds number
V	flow velocity in main channel
W	width of channel
W_s	width of slot between plate and each side of channel

$X_{l.e.}$ distance from elastic axis to leading edge of plate, measured in plate lengths

X_{α} distance from elastic axis to center of mass, measured in plate lengths

α pitching angle of plate

$\beta = (W - W_s)/W$

$\zeta_h = C_h/[2m(W - 2W_s)\omega_{nh}]$, damping ratio for translational motion

$\zeta_{\alpha} = C_{\alpha}/[2I_{\alpha}(W - 2W)\omega_{n\alpha}]$, damping ratio for pitching motion

ν kinematic viscosity

ρ fluid density

$\sigma = H/(H - a)$

ω critical frequency

$\omega_{nh} = [K_h/m(W - 2W_s)]^{1/2}$, natural frequency in translation

$\omega_{n\alpha} = [K_h/I (W - 2W_s)]^{1/2}$, natural frequency in pitching

ANALYSIS

Because of the large number of parameters affecting plate vibrations in narrow channels, there may be several conceivable mechanisms by which the vibrations might be excited. Theories based on each of the mechanisms presumably can predict a different range of critical flow velocities and different effects when some of the parameters are varied.

In order to gain an understanding of the mechanisms involved in these self-eccited vibrations, Bland, et al. (ref. 4), of NASA-Langley Research Center conducted a series of tests with the apparatus similar to the one shown schematically in Figure 1. In their idealized flow channel, the width of the plate was nearly equal to the width of the channel, and, hence, the flow was nearly two-dimensional. They found that the plate would begin to vibrate only for airspeeds above some critical value, but, that once begun, the vibrations would persist for airspeeds lower than the critical value until at some even lower speed the vibrations would stop. These "starting" and "stopping" speeds were almost equal for small channel heights. The critical speed decreased as the channel height decreased, but, below a
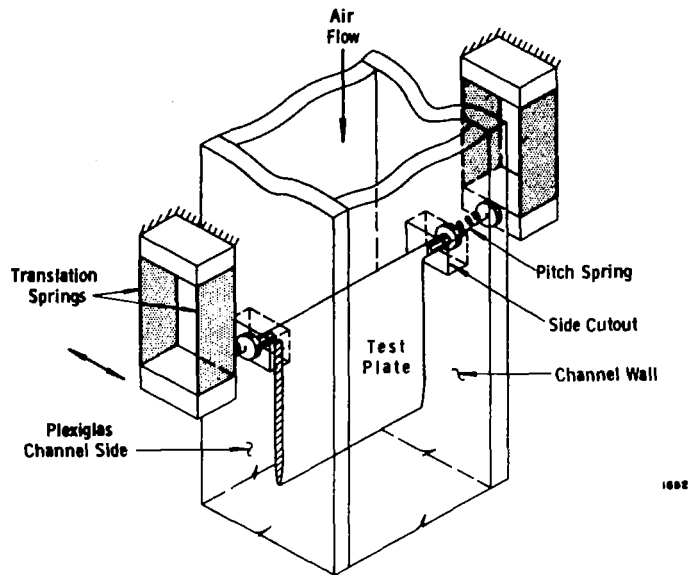
4

FIGURE 1. —LANGLEY RESEARCH CENTER APPARATUS

small enough height, the speed increased substantially, which was tentatively explained as due either to viscosity or the flow around the sides of the plate in the gap between the plate and the channel walls. They also presented a theory for inviscid, incompressible linearized flow in a channel which involved an extension of the kernel function analysis of wall effects on a two-dimensional oscillating wing in a wind tunnel (ref. 5). For most of the tests, it was concluded that the theory gave reasonable agreement down to ratios of channel height to plate length of about 0.2. For ratios less than 0.2, the theory did not agree with the experimental tests.

· Miller and Kennison (ref. 2) conducted a series of tests of narrow channel, flow-induced vibrations with an apparatus shown schematically in Figure 2. Their analysis included viscous effects but not cross flow around the sides of the plate. As mentioned earlier, their theoretical results did not agree with their experimental tests, but they did show that less flow is required to induce the vibrations as the depth of insertion of the blade into the scabbard is reduced.
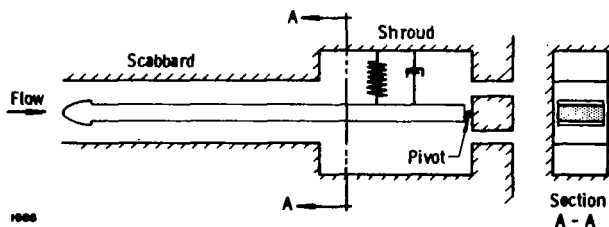

FIGURE 2. —KNOLLS ATOMIC POWER LABORATORY APPARATUS

5

The plate vibrations in both of the setups shown in Figures 1 and 2 were of the self-excited type. For some other range of the parameters, however, a high frequency vibration might be excited by vortex shedding in which the trailing edge geometry of the plate plays a large part; but this type of excitation should not be important for small channel height-to-plate length ratios although it is important for flows across elastic structures such as heat exchanger tube bundles (refs. 6, 7). Also, in some cases, turbulent fluctuations may cause a low level vibration. Consequently, the purpose of the analysis presented here was to discover if a hydraulic flow theory, neglecting vortex shedding and turbulence "noise," would be sufficient to predict accurately the critical flow velocity for ratios of channel height to plate length less than about 0.2, for which potential flow theories are known not to be applicable.

A one-dimensional theory allows viscosity, energy losses at abrupt changes in the channel area, and plate thickness all to be taken into account; but neither the hydrodynamic loads nor the flow split between the upper and lower channels can be calculated as precisely as in the potential flow flutter approximation. Nonetheless, both theories are similar inasmuch as they are not response analyses but rather hydroelastic analyses in which the vibrating plate influences the hydrodynamic loading, and vice versa.
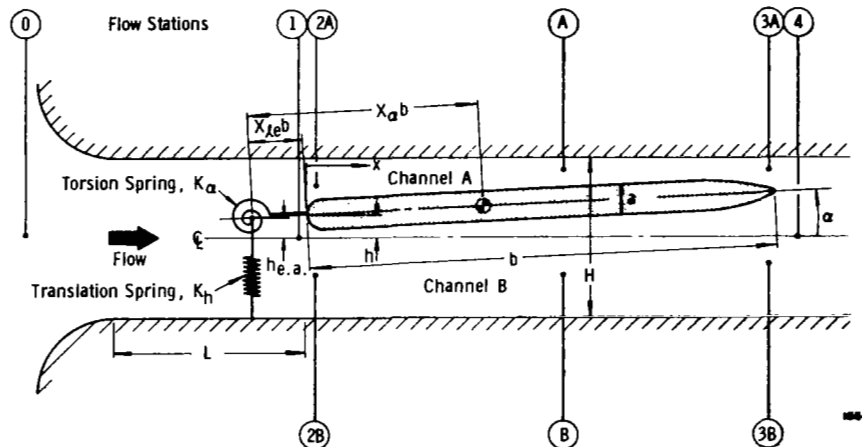
FIGURE 3.—SCHEMATIC OF FLOW CHANNEL

The general flow geometry is sketched in Figure 3. A plate of length b and thickness a is elastically suspended by torsion and translation springs in a flow channel of height H. The width of the channel is W; there is a gap of width W_s between the plate and each side of the channel so the width of the plate itself is $W - 2W_s$. The distance from the elastic axis of the springs to the center of the translating mass is $X_a b$, and the distance to the leading edge of the plate is $X_{l.e.} b$. (In the Langley Research Center

6

apparatus, the test channel stands vertically and is connected to a vacuum chamber downstream of the plate. Temperature controlled room air flows through the channel to the vacuum chamber, with the flow rate being controlled by a downstream valve. A bell mouth entrance to the channel and a long entrance L are used to provide uniform flow at the plate location.) *error*

For the purposes of analysis, a number of flow stations are erected in the channel, as shown in Figure 3. Downstream locations are measured in an x-coordinate axis fixed at the centerline of the channel at the point where the leading edge of the plate intersects it when the plate is centered in the channel. The translation of the leading edge from the centerline of the channel is denoted by h and the pitching angle by α. The method of analysis is to determine the pressure, $\overline{P}$, and velocity, $\overline{V}$, at each of the flow stations in terms of the unknowns h and α and then use these pressures and velocities in the equations of motion for the plate to determine h and α as a function of time. In general, h and α will have nondecaying amplitudes only if $\overline{V}$ is greater than some critical value.*

For a given total pressure drop, $P_0 - \overline{P}_4$, the average velocity $\overline{V}$ in the main channel upstream of the plate may vary as the plate moves about in the channel; likewise, a constant $\overline{V}$ may cause a varying $P_0 - \overline{P}_4$. Thus, both $\overline{V}$ and $\overline{P}_4$, in general, may be time varying, and this fact should be included in the analysis. (It should be noted that in classical flutter analyses the flow approaching the plate is assumed to be constant.)

The viscous forces or energy dissipation in the flow are calculated by using friction factors and loss coefficients which depend on the Reynolds number. Thus, at station 1, just ahead of the leading edge of the plate, the average pressure across the channel is

$$\overline{P}_1 = P_0 - \frac{1}{2}\rho\overline{V}^2\left(K_0 + \overline{F}_0\frac{L}{\mathscr{D}_0}\right) - \rho L\frac{d\overline{V}}{dt} \tag{1}$$

In Eq. (1), K_0 is the pressure-drop coefficient for the entrance from the atmosphere ($K_0 \geq 1$; it equals one only for a smoothly streamlined entrance), and $\overline{F}_0$ is the friction factor for fully developed flow in the channel based on the instantaneous Reynolds number, $\overline{V}\mathscr{D}_0/\nu$, where $\mathscr{D}_0$ is the hydraulic diameter, $2HW/(H + W)$. Furthermore, the average mass-flow velocity and the average momentum-flow velocity are assumed to be approximately equal. Unsteady velocity profiles are not known accurately enough, anyway, to enable the analysis to be made more exact. Likewise, a friction factor based on a steady velocity equal to the instantaneous velocity is used because of the lack of any convenient data on friction factors for unsteady flow.

---

*A bar over a symbol indicates that that quantity may vary with time.

At station 2A, the energy equation for the part of the flow entering channel A is

$$\overline{P}_{2A} = \overline{P}_1 - \frac{1}{2}\rho\left[(\overline{K}_{LA} + 1)\overline{V}_{2A}^2 - \overline{V}^2\right] \tag{2}$$

where $\overline{K}_{LA}$ is the loss coefficient for the channel contraction. The height of channel A at the leading edge of the plate is approximately

$$\overline{H}_{2A} = \frac{1}{2}(H - a\cos\alpha) - h \tag{3}$$

Conservation of flow at the leading edge gives one relation for determining the flow-split between channels A and B; it is

$$\overline{V}_A\overline{H}_{2A} + \overline{V}_B\overline{H}_{2B} = \overline{V}H \tag{4}$$

Now, concentrating on an arbitrary point in the interior of channel A, the integrated form of conservation of flow for the control volume spanning channel A (Figure 4) is

$$\frac{d}{dt}(\overline{m}_{cv}) = (\text{mass flow})_{in} - (\text{mass flow})_{out}$$

Evaluating these terms for the indicated infinitesimal control volume, and letting the size of the control volume vary as dictated by the plate motion, the differential form of conservation of flow in channel A is seen to be:

$$\overline{H}_A\frac{\partial\overline{V}_A}{\partial x} - \overline{V}_A\tan\alpha + \frac{2\overline{Q}_{AB}}{W - 2W_s} = -\frac{dH_A}{dt} \tag{5}$$

where $\overline{Q}_{AB}$ is the cross flow from channel A to channel B through the slots, per unit length of the plate, and the channel height, $\overline{H}_A$, is approximately

$$\overline{H}_A = \frac{1}{2}(H - a\cos\alpha) - h - x\tan\alpha \tag{6}$$
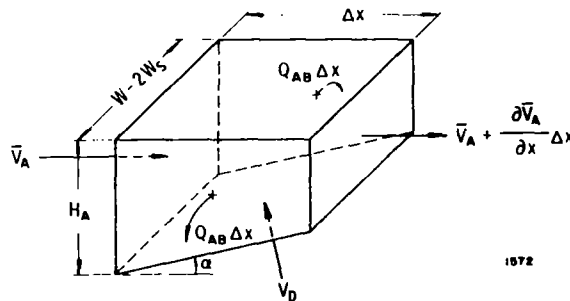
FIGURE 4.—CONTROL VOLUME FOR FLOW CONSERVATION

Calculating the cross-flow relationships between the pressure drop across the channels and the flow through the channels is a difficult problem which is still unsolved analytically. Thorpe (ref. 8) gives a good review of the work that has been done and recommends computing the "jet" velocity, $\overline{V}_{AB}$ (Figure 5) by assuming it is equal to the velocity in channel A after being accelerated through the pressure drop $\overline{P}_A - \overline{P}_B$, or, in other words,

$$\overline{V}^2_{AB} = \overline{V}^2_A + 2(\overline{P}_A - \overline{P}_B)/\rho \tag{7}$$

Then $\overline{Q}_{AB}$ is given by $\overline{V}_{AB}$ multiplied by the flow area normal to the velocity, or

$$\overline{Q}_{AB} = C_D W_s \overline{V}_{AB} \tan \alpha \tag{8}$$

where C_D accounts for the jet width, W_j, not being equal to the slot width, W_s.
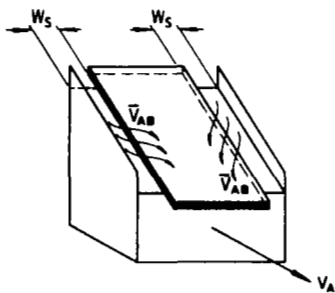
FIGURE 5. — CROSS FLOW
THROUGH SLOTS
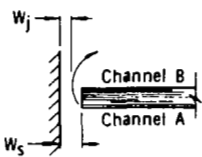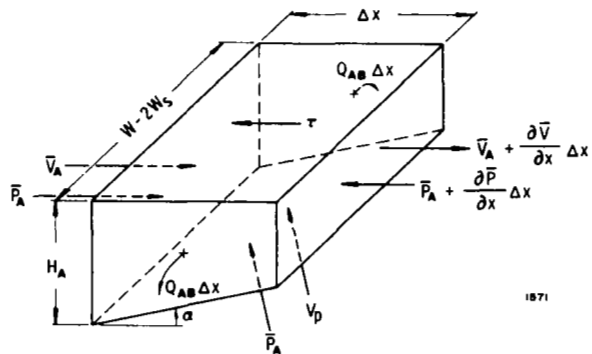
FIGURE 6. — CONTROL VOLUME FOR
MOMENTUM CONSERVATION

The integrated form of the conservation of momentum for a control volume spanning channel A (Figure 6) is

$$\sum (\text{forces})_x = \frac{d}{dt}(\overline{m}_{cv} \overline{V}_A) + (x\text{ - momentum flow})_{out} - (x\text{ - momentum flow})_{in}$$

By letting the control volume become infinitesimal and taking into account the varying size of the control volume, the differential form of conservation of momentum for channel A becomes

$$\frac{1}{\rho}\left(\frac{\partial \overline{P}_A}{\partial x}\right) + \frac{\overline{F}_A \overline{V}^2_A}{2\overline{D}_A} + \overline{V}_A \frac{\partial \overline{V}_A}{\partial x} + \frac{2\overline{Q}_{AB}(\overline{V}_{AB} - \overline{V}_A)}{\overline{H}_A(W - 2W_s)} + \frac{\partial \overline{V}_A}{\partial t} = 0 \tag{9}$$

9

The viscous shear stresses are based on a friction factor, $\overline{F}_A$, through the Darcy-Weisbach relation $\overline{\tau}_A = \rho \overline{F}_A \overline{V}_A^2 / 8$. The hydraulic diameter, $\mathscr{D}_A = 2\overline{H}_A W / (\overline{H}_A + W - W_s)$, is based on a flow area of $\overline{H}_A W$ and an average wetted perimeter of $2\overline{H}_A + W + (W - 2W_s)$; the cross flow $\overline{Q}_{AB}$ is assumed to leave the control volume with a velocity of $\overline{V}_{AB}$ in the x-direction.

The frictional pressure drop in the short trailing edge region near station 3A is not calculated explicitly but is assumed to be given accurately enough by the preceding equation. The pressure in channels A and B is taken to be equal at the exit plane similarly to what is done in potential flow around airfoils (the Kutta condition). Experiments have verified this to be true even for viscous flows (ref. 8). Thus

$$\overline{P}_{3A} = \overline{P}_{3B} = \overline{P}_3 \tag{10}$$

The trailing edge is sufficiently streamlined that exit energy losses can be ignored. Then an energy balance on the two merging streams yields

$$\overline{P}_3 - \overline{P}_4 = \frac{1}{2}\rho \left[\overline{V}^2 - \frac{\overline{H}_{3A}\overline{V}_{3A}^3}{H\overline{V}} - \frac{\overline{H}_{3B}\overline{V}_{3B}^3}{H\overline{V}} \right] \tag{11}$$

where the channel height $\overline{H}_{3A}$ is

$$\overline{H}_{3A} = \frac{1}{2}(H - a\cos\alpha) - h - b\tan\alpha \tag{12}$$

Conservation of flow requires

$$\overline{V}_{3A}\overline{H}_{3A} + \overline{V}_{3B}\overline{H}_{3B} = \overline{V}H \tag{13}$$

It is the equating of the pressures $\overline{P}_{3A}$ and $\overline{P}_{3B}$ at the exit plane that allows the flow-split around the leading edge of the plate to be determined. In other words, without Eq. (10), there are twenty unknowns [assuming P_0, $\overline{P}_4$, h(t), and α(t) are known] and only nineteen equations (including the similar equations for channel B).

The above equations and the two equations of motion for the plate allow the critical velocity to be calculated, in principle. However, the concern here is only with the onset of sustained vibrations, so by assuming the amplitude of the vibrations are small the equations can be linearized. This allows the critical velocity to be determined much more easily since, after linearization, all the flow equations and the hydrodynamic loads can be integrated analytically.

Linearization of Flow Equations

Now, all the parameters with bars over them are assumed to be of the form

$$\overline{E}(x, t) = E(x) + e(x, t) \qquad (14)$$

where $E(x)$ is the steady state value of $\overline{E}$ obtained when the plate is at rest in the center of the channel and $e(x, t)$ is a small fluctuation of the order of magnitude of $a(t)$ or $h(t)$. Furthermore, it is assumed that $|e/E| << 1$.

The complete set of linearized equations is given in Appendix A, but there are several points in the linearization that should be discussed. In Eq. (1), K_O is assumed to be determined by the inlet geometry of the main channel so it is not a function of Reynolds number. Furthermore, $\overline{F}_O$ is assumed to be given accurately enough by the following correlation equations (ref. 9):

$$\overline{F}_O = \frac{T}{(N_{Re})^n} \begin{cases} T = 64, & n = 1 & \text{for} & 0 \leq N_{Re} \leq 1829 & (15a) \\[2mm] T = 0.035, & n = 0 & \text{for} & 1829 \leq N_{Re} \leq 6645 & (15b) \\[2mm] T = 0.316, & n = \frac{1}{4} & \text{for} & N_{Re} \geq 6645 & (15c) \end{cases}$$

Equations (15a, c) are for laminar and turbulent flow, respectively, although Eq. (15c) holds exactly only for $N_{Re} < 100,000$ (ref. 9). Further, these are for circular pipes, but, by using the equivalent hydraulic diameter, they are adequate for noncircular cross sections, especially in the turbulent regime. Equation (15b) approximates the transitional flow regime by a constant friction factor of 0.035. Using these equations, the unsteady friction factor f_O works out to be

$$f_O = -nF_O(v/V)$$

where F_O is the constant friction factor for the steady velocity V. This relation, as mentioned previously, is based on the assumption that $\overline{F}_O = F_O + f_O$ is equal to a friction factor based on a steady flow equal to $\overline{V} = V + v$.

In Eq. (2), the steady state loss coefficients in channels A and B are equal, $K_{LA} = K_{LB} = K_L$. The unsteady loss coefficient, k_{LA}, is based on a steady flow through a constant channel contraction equal to the instantaneous contraction determined by h and a. Even with this assumption, however, there seem to be no existing data which could be used to indicate precisely how k_{LA} ought to vary with a; that is, loss coefficients are usually given only for parallel channels. Yet experiments with inclined plates in steady flow show that the extra flow separation (Figure 7) in the diverging channel leads to loss coefficients half again as large as might be expected for the same area reduction in parallel channels (ref. 8). Furthermore,
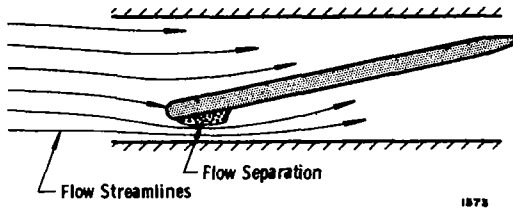
FIGURE 7. —FLOW SEPARATION IN DIVERGING CHANNEL

this part of the loss is nonsymmetrical as there is no corresponding loss in the converging channel. Because of this fact and the lack of any real data, it is assumed here that the angular variation of k_L in the diverging channel is equal to half the variation caused by a parallel reduction equal to $b\alpha$. Thus,

$$\overline{K}_{LA} = K_L + \left[h + \frac{1}{2}U\langle - \alpha\rangle b\alpha\right]\frac{dK_L}{dh}$$

where dK_L/dh can be evaluated from existing tables of loss coefficients (refs. 9, 10). $U\langle\alpha\rangle$ is the unit step function defined as

$U\langle\alpha\rangle = 0$ for $\alpha < 0$

$U\langle\alpha\rangle = 1$ for $\alpha > 0$

In Eq. (8), the cross flow $\overline{Q}_{AB}$ after linearization is

$Q_{AB} = 0$

and

$$q_{AB} = K_D W_s V_A \alpha$$

since $\overline{V}_{AB}$ differs from V_A only by terms of the order of α or h. Also, because of the symmetry of flow when the plate is at rest in the center of the channel, the steady flow velocities in channels A and B are equal, $V_A = V_B = \sigma V$. Hence, q_{AB}, in this linearized form, merely represents the portion of the undisturbed main flow crossing from one channel to the other because of the inclination of the plate. This is probably a very crude approximation to the actual cross flow, but it is likely to be the best that can be done using a hydraulic theory.

In Eq. (9), the unsteady part of $\overline{F}_A\overline{V}_A^2 /\overline{\mathscr{D}}_A$ has contributions from all of $\overline{F}_A$, $\overline{V}_A$, and $\overline{\mathscr{D}}_A$. All of these variations are taken into account, although once again $\overline{F}_A = F_A + f_A$ is set equal to a friction factor based on a steady flow of $V_A + v_A$ and a constant hydraulic diameter of $\overline{\mathscr{D}}_A = \mathscr{D}_A + d_A$.

Correlation equations similar to those used for $\overline{F}_O$ are used to compute F_A and f_A; the pertinent Reynolds number here is $N_{Re} = \sigma V \mathscr{D}_A / \nu$.

Finally, the linearized analysis shows that the unsteady pressure, p_4, is a linear function of the unsteady velocity v in the main channel plus a function proportional to $U\langle a \rangle\, badC_L/dh$, the loss coefficient for angular variations in the channel height. Considering that this loss coefficient is computed in a rather arbitrary way, it is neglected in calculating p_4. Thus, p_4 does not depend explicitly on either h or a, and no contradiction is implied by setting both p_4 and v equal to zero. In other words, if the pressure drop $P_0 - \overline{P}_4$ is constant ($p_4 = 0$), then the linearized analysis says that $v = 0$; likewise, if $v = 0$ then p_4 must be zero. Consequently, both p_4 and v are put equal to zero in what follows, although, for vibrations of finite amplitude, either $\overline{P}_4$ or $\overline{V}$ must be allowed to vary.

Linearized Equations of Motion for Vibrating Plate

The linearized torsional equation of motion for the plate is

$$(W - 2W_s)I_a \ddot{a} + C_a \dot{a} + K_a a + (W - 2W_s)mX_a b \ddot{h}_{e.a.}$$

$$= (W - 2W_s)\left\{ \int_0^b \frac{1}{2}a(\tau_B - \tau_A)dx + \int_0^b [bX_{\ell.e.} + x](p_B - p_A)dx \right\} \quad (16)$$

where τ_A is the linearized shearing stress on the side of the plate facing channel A and likewise for τ_B.

The linearized translational equation of motion is

$$(W - 2W_s)m[\ddot{h}_{e.a.} + X_a b \ddot{a}] + C_h \dot{h}_{e.a.} + K_h h_{e.a.}$$

$$= (W - 2W_s)\int_0^b (p_B - p_A)dx \quad (17)$$

where $h_{e.a.} = h - X_{\ell.e.}ba$.

By substituting the relations for τ_A, τ_B, p_A, and p_B given in Appendix A into Eqs. (16) and (17) and by assuming that $h = h_o \exp(i\omega t)$ and $a = a \exp(i\omega t)$, the problem of determining V and ω can be reduced to the simultaneous solution of two algebraic, homogeneous equations. The equations are of the form

$$(A_{1a} + iB_{1a})a_o + (A_{1h} + iB_{1h})\frac{h_o}{b} = 0 \quad (18)$$

13

and

$$(A_{2\alpha} + iB_{2\alpha})a_o + (A_{2h} + iB_{2h})\frac{h_o}{b} = 0 \qquad (19)$$

Equation (18) is derived from Eq. (16), and Eq. (19) from Eq. (17). The A's and B's are functions of the unknown velocity V and the unknown frequency ω as shown in Appendix A. Thus, Eqs. (18) and (19) can be solved numerically for the values of V and ω that allow a_o and h_o to take on nonzero values. These, then, are the critical velocity and the flutter frequency.

RESULTS

In order to determine the range of validity of the theory, comparisons between it and existing experimental data (ref. 4) were made for two distinct flow situations: a plate 2 in. long contained in a channel of variable height, and a plate 1 in. long contained in the same channel. In both cases, the parameter varied was the channel height, H. The computer program used in solving Eqs. (18) and (19) to obtain numerical results is described in Appendix B.

Figure 8 shows results for the 2-in. long plate (Plate 2A of ref. 4) having the mass distribution described in the figure. To facilitate direct comparison with the experimental data, the velocity given in the figure is that in the reduced channel between the plate and the walls; this velocity is larger than the velocity V in the unobstructed channel by the multiplicative factor σ. Results from the potential flow theory mentioned earlier are also shown to help illustrate the influence of viscosity and other flow losses.

The one-dimensional, hydraulic flow theory is in qualitative agreement with the potential flow theory for the range of channel heights shown; that is, both the critical velocity and critical frequency decrease as the channel height spacing decreases. The hydraulic flow results do not, however, agree with experimental results for very small channel heights, for which the critical velocity and frequency increase markedly. For larger channel heights (but still for H/b < 0.2), the present theory is in reasonable agreement with experiment, especially with regard to the critical frequency.

In the hope of gaining further insight into the physical mechanisms involved, the higher order roots of Eqs. (18) and (19) were also investigated. In addition to the lowest velocity roots shown in Figure 8 by the solid curve, the roots corresponding to the second lowest critical velocity and frequency are also shown for H < 0.1. As can be seen, the velocity and frequency for this "second mode" increase as the channel height decreases in much the same way as the experimental data do.

14
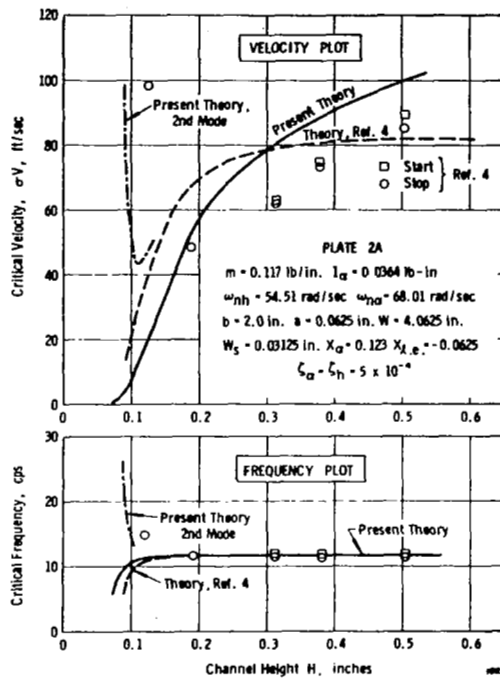
FIGURE 8. — COMPARISON OF THEORY AND EXPERIMENT
FOR NASA PLATE 2A

Comparisons for a 1-in. long plate (Plate 1B of ref. 4) are shown in
Figure 9. Again the results are in fair agreement with potential flow theory
for $H/b < 0.2$, but once more the theory does not predict the observed increase
in critical velocity and frequency for small channel heights. Results of cal-
culations for the second mode for this plate are also shown on the figure.
(Note that a channel height of 0.2 in. corresponds to $H/b = 0.2$ for Plate 1B
while a channel height of 0.4 in. corresponds to $H/b = 0.2$ for Plate 2A. Thus,
it can be seen that for $H/b < 0.2$ the present theory and the potential flow
theory are in good agreement but that for larger values of H/b the present
results greatly overestimate the critical velocity; this checks with the previous
remarks that the hydraulic flow assumption would be tenable only for small H/b.)

For neither of the plates is there a true nodal point for the flow-
induced vibration (since the plate does not vibrate in a natural mode), but, in
both cases, the phase angle between the pitch and translation motion is so
small, according to the theory, that the plate appears to rotate about a

15
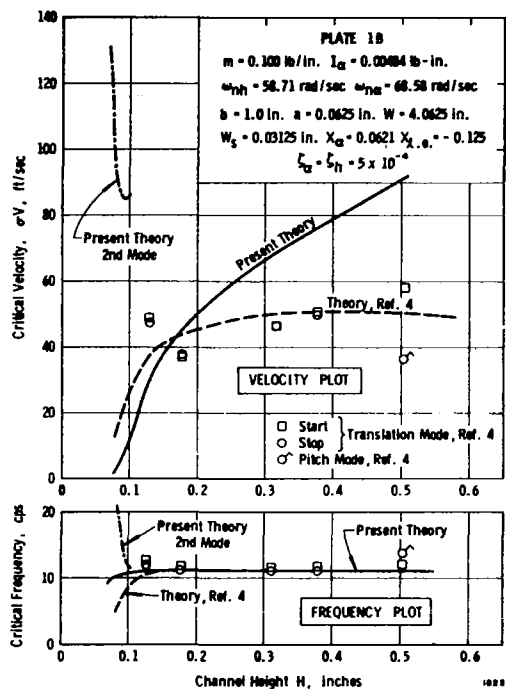
FIGURE 9. — COMPARISON OF THEORY AND EXPERIMENT
FOR NASA PLATE 1B

point ahead of the plate during most of any one cycle. This predicted "trans-
lation" mode agrees with the experiments. However, for plate 1B only, a
"pitch" mode (rotation point near plate mid-chord) was also observed experi-
mentally for large channel heights; at the "starting" velocity, the mode was
always translation, but, as the flow rate decreased, the apparent axis of
rotation would shift rearward, and, at the "stopping" velocity, the plate oscil-
lated in a pitch mode; one such point is shown flagged in Figure 9. Neither
the hydraulic theory presented here nor the potential flow theory of ref. 4
predicts such a mode.

The validity of the approximate method of calculating the cross flow
could not be checked since the experimental tests were deliberately designed
to be very nearly two-dimensional; that is, neither of the two plates were
sufficiently narrow nor the slots between the sidewalls and the plate suf-
ficiently large to influence the flow appreciably. However, when the slots
are larger [actually, when the parameter $2C_D W_s/(W - 2W_s)$ is comparable
to unity], the critical velocity, according to the theory, must increase if the
other plate parameters are held constant.

In order to determine how great a role the inertia of the fluid plays
in narrow channel oscillations, the fluid velocity and pressures were also
calculated by a quasi-steady method in which only the instantaneous position
of the plate (and not its velocity or acceleration) determined the flow. The

16

governing equations can be derived by setting $\dot{a} = \ddot{a} = \dot{h} = \ddot{h} = 0$ in the fluid dynamic theory given in the preceding sections. This quasi-steady theory did not predict flow-induced vibrations for any of the cases tested. However, for some cases, as for example when the elastic axis is behind the mid-chord point of the plate, a divergence may be predicted.

CONCLUSIONS

The results of the analysis presented here show that viscous effects and energy losses, at least when calculated by the approximations implied in a one-dimensional hydraulic flow theory, are not sufficient to explain the experimentally observed increase in the flow velocity required to induce vibrations of a plate contained in a flow channel when the channel height is made very small. In fact, the relatively good agreement of the hydraulic flow theory and previous potential flow calculations for $H/b < 0.2$ indicates that fluid inertia forces predominate in both theories. There are, however, slight differences between the two theories since the hydraulic flow theory predicts a slightly smaller critical velocity than does the potential flow theory for small H/b ratios. This presumably is caused by viscous effects and other energy losses although ordinarily it might be expected that an increase in energy losses (or damping) should lead to an increase in the critical velocity; the reason for the decrease, then, must be an even more significant change in the relative phase angles between the various flow forces.

Because of the lack of correlation between theory and experiment, it is still not clear what causes the rapid increase in the critical flow velocity for very small H/b. However, the qualitative agreement between the theoretical computations for the second mode of vibration for these cases and the experimental observations may imply that possible large increases in nonlinear effects for such small channel heights add enough additional stability to make vibrations in the lowest frequency mode so small as not to be observable. On the other hand, these same nonlinearities, if they do exist, could change the characteristics of the finite-amplitude vibrations of the lowest order mode sufficiently to reconcile them with experiment. Finally, even though the vibrations may be linear, the balance of viscous, inertia, and other forces might be so subtle for small H/b that a much more exact viscous flow theory is required here.

Further analytical and experimental research on narrow channel flow-induced vibrations is clearly indicated. Closer correlation of theory and experiment for all conditions will be realized only when more realistic flow theories are used (e.g., unsteady boundary layer flow); furthermore, it may also prove necessary to include nonlinear effects.

Southwest Research Institute
San Antonio, Texas
March 11, 1968

APPENDIX A. LINEARIZED EQUATIONS

Steady-Flow Equations

When $a = \dot{a} = \ddot{a} = h = \dot{h} = \ddot{h} = 0$, the "steady-flow" pressure drops and velocities are

$$P_0 - P_{2A} = P_0 - P_{2B} = \frac{1}{2} \rho V^2 \left[K_o + F_o \frac{L}{\mathcal{D}_o} + (C_L + 1)\sigma^2 - 1 \right]$$

$$P_0 - P_{3A} = \frac{1}{2} \rho V^2 \left[K_o + F_o \frac{L}{\mathcal{D}_o} + (K_L + 1)\sigma^2 - 1 + \sigma^2 \beta F \frac{b}{\mathcal{D}} \right] = P_0 - P_{3B}$$

$$P_0 - P_4 = \frac{1}{2} \rho V^2 \left[K_o + F_o \frac{L}{\mathcal{D}_o} + \sigma^2 K_L + \sigma^2 \beta F \frac{b}{\mathcal{D}} \right]$$

and

$$V_A = V_B = \sigma V$$

Unsteady-Flow Equations

The unsteady flow pressures and velocities are derived on the assumption that products of a, h, v_A, and v_B may be neglected in comparison to linear terms. The results are

$$P_{2A} \Big/ \frac{1}{2} \rho V^2 = - 2\sigma^2 (K_L + 1) \frac{v_{2A}}{V} - \sigma^2 A C_{Lh} \frac{h}{b} - \frac{1}{2} \sigma^2 A C_{Lh} (1 - U\langle a \rangle) a$$

$$P_{2B} \Big/ \frac{1}{2} \rho V^2 = - 2\sigma^2 (K_L + 1) \frac{v_{2B}}{V} + \sigma^2 A C_{Lh} \frac{h}{b} - \frac{1}{2} \sigma^2 A C_{Lh} U\langle a \rangle a$$

where

$$K_{Lh} = H \frac{dK_L}{dh}$$

$$\frac{P_A}{1/2(\rho V^2)} = \frac{P_{2A}}{1/2(\rho V^2)} - \frac{2x\dot{v}_{2A}}{V^2} - (2-n)\sigma\beta F \frac{x}{\not{\beta}}\left(\frac{v_{2A}}{V}\right) - \left[(2-n)\sigma^2\beta F \frac{x^2}{H\not{\beta}} + \right.$$

$$\left. + 4\sigma^2 \frac{x}{H}\right]\frac{\dot{h}}{V} - 2\sigma\frac{x^2\ddot{h}}{V^2} - \left[(2-n)\left(1 - \frac{2K_D W_s}{W - 2W_s}\right)\sigma^3\beta F \frac{x^2}{H\not{\beta}} + \right.$$

$$\left. + (1+n)\sigma^4\beta^2 F \frac{x^2}{H^2} + 4\left(1 - \frac{2K_D W_s}{W - 2W_s}\right)\sigma^3 \frac{x}{H}\right]\alpha - \left[\frac{1}{3}(2-n)\sigma^2\beta F \frac{x^3}{H\not{\beta}} + \right.$$

$$\left. + 2\sigma^2 \frac{x^2}{H} + 2\left(1 - \frac{2K_D W_s}{W - 2W_s}\right)\sigma^2 \frac{x^2}{H}\right]\frac{\dot{\alpha}}{V} - \frac{2}{3}\sigma\frac{x^3\ddot{\alpha}}{V^2}$$

A similar equation holds for p_B with α and h replaced by $-\alpha$ and $-h$ and the subscripts A replaced by B. The linearized shear stress on the plate is

$$\tau_A = -\frac{1}{8}\sigma\beta F V^2(2-n)\frac{v_A}{V} + \frac{1}{4}\sigma^4 n F V^2\beta^2 \frac{\not{\beta}}{H}\left(\frac{h + x\alpha}{H}\right)$$

where

$$v_A = v_{2A} + \frac{2\sigma}{H}\left(x\dot{h} + \frac{1}{2}x^2\dot{\alpha}\right) + 2\sigma^2\left(1 - \frac{2K_D W_s}{W - 2W_s}\right)\left(\frac{x\alpha}{H}\right)V$$

Similar equations hold for τ_B and v_B.

Equating p_{3A} to p_{3B} yields $v_{2B} = -v_{2A}$ and the flow-split equation

$$\frac{\dot{v}_{2A}b}{V^2} + \sigma\left[K_L + 1 + \frac{1}{2}(2-n)\beta\mathcal{F}\right]\frac{v_{2A}}{V} = -\left[(1+n)\sigma^4\beta^2 A^2 F + \right.$$

$$\left. + \frac{1}{2}\sigma^2 A K_{Lh}\right]\frac{h}{b} - \left[\frac{1}{2}(2-n)\sigma^2\beta A\mathcal{F} + 2\sigma^2 A\right]\frac{\dot{h}}{V} - \sigma A \frac{b\ddot{h}}{V^2} - \right.$$

$$-\left[\frac{1}{2}(2-n)\left(1 - \frac{2K_D W_s}{W - 2W_s}\right)\sigma^3\beta A\mathcal{F} + \frac{1}{2}(1+n)\sigma^4\beta^2 A^2 F + \right.$$

$$\left. + 2\sigma^3 A\left(1 - \frac{2K_D W_s}{W - 2W_s}\right) + \frac{1}{8}\sigma^2 A C_{Lh}\right]\alpha - \left[\frac{1}{6}(2-n)\sigma^2\beta A\mathcal{F} + \right.$$

$$\left. + \left(2 - \frac{2K_D W_s}{W - 2W_s}\right)\sigma^2 A\right]\frac{b\dot{\alpha}}{V} - \frac{1}{3}\sigma A \frac{b^2\ddot{\alpha}}{V^2}$$

20

By letting $v_{2A} = v_o e^{i\omega t}$, $a = a_o e^{i\omega t}$, and $h = h_o e^{i\omega t}$, Eqs. (16) and (17) of the section, Analysis, reduce to

$$(A_{1a} + iB_{1a})a_o + (A_{1h} + iB_{1h})\frac{h_o}{b} = 0 \tag{A1}$$

and

$$(A_{2a} + iB_{2a})a_o + (A_{2h} + iB_{2h})\frac{h_o}{b} = 0 \tag{A2}$$

where

$$A_{1a} = \frac{1}{8}\beta F\left(\frac{a}{b}\right)\left(\frac{\rho b^4}{I_a}\right)\left(\frac{V}{b\omega_{na}}\right)^2\left[(2-n)\sigma V_{ar} + (2-n)\sigma^3 AK + \right.$$

$$+ \sigma^4 n\beta A \frac{\cancel{B}}{H}\Bigg] + \left(\frac{\rho b^4}{I_a}\right)\left(\frac{V}{b\omega_{na}}\right)^2\left(\frac{V}{b\omega}\right)^2\sigma AG\Bigg\{2\sigma^3\Bigg[K_L + 1 +$$

$$+ \frac{1}{2}(2-n)\beta\mathcal{F}\Bigg]\left\{(K_L+1)\left[\frac{1}{3}(2-n)\sigma\beta\mathcal{F}K\left(X_{\ell.e.}+\frac{1}{3}\right)-\right.\right.$$

$$-\frac{1}{8}K_{Lh}\left(X_{\ell.e.}+\frac{1}{2}\right)+\frac{1}{3}(1+n)\sigma^2\beta^2 AF\left(X_{\ell.e.}+\frac{3}{8}\right)+$$

$$+ \sigma K\left(X_{\ell.e.}+\frac{1}{3}\right)\Bigg] + \frac{1}{2}(2-n)\beta\mathcal{F}\left[\frac{1}{12}(2-n)\sigma\beta\mathcal{F}K\left(X_{\ell.e.}+\frac{1}{2}\right)+\right.$$

$$+\frac{1}{12}(1+n)\sigma^2\beta AF\left(X_{\ell.e.}+\frac{1}{3}\right)-\frac{3}{16}K_{Lh}\left(X_{\ell.e.}+\frac{4}{9}\right)\Bigg]\Bigg\}+$$

$$+ 2\sigma\left(\frac{b\omega}{V}\right)^2\left\{\frac{1}{2}\sigma(K_L+1)\left(X_{\ell.e.}+\frac{1}{3}\right)\left[\frac{1}{6}(2-n)\beta\mathcal{F}+1+K\right]+\right.$$

$$+\frac{1}{12}(2-n)\sigma\beta\mathcal{F}K\left(X_{\ell.e.}+\frac{1}{2}\right)+\frac{1}{12}(1+n)\sigma^2\beta^2 AF\left(X_{\ell.e.}+\frac{1}{2}\right)-$$

$$-\sigma\left[K_L+1+\frac{1}{2}(2-n)\beta\mathcal{F}\right]\left[\frac{1}{4}(K_L+1)\left(X_{\ell.e.}+\frac{2}{5}\right)+\right.$$

$$+\frac{1}{24}(2-n)\beta\mathcal{F}\left(X_{\ell.e.}+\frac{8}{15}\right)\Bigg]-\frac{3}{16}K_{Lh}\left(X_{\ell.e.}+\frac{4}{9}\right)\Bigg\}-$$

$$-\frac{1}{6}\left(X_{\ell.e.}+\frac{8}{15}\right)\left(\frac{b\omega}{V}\right)^4\Bigg\}+1-\left(\frac{\omega}{\omega_{na}}\right)^2\left[1-\left(\frac{mb^2}{I_a}\right)X_a X_{\ell.e.}\right]$$

$$B_{la} = 2\zeta_a \left(\frac{\omega}{\omega_{na}}\right) + \frac{1}{8}\beta F\left(\frac{a}{b}\right)\left(\frac{\rho b^4}{I_a}\right)\left(\frac{V}{b\omega_{na}}\right)^2\left[(2-n)\sigma v_{ai} + \right.$$

$$\left. + \frac{1}{3}(2-n)\sigma^2 A\left(\frac{b\omega}{V}\right)\right] + 2\left(\frac{\rho b^4}{I_a}\right)\left(\frac{V}{b\omega_{na}}\right)^2\left(\frac{V}{b\omega}\right)\sigma^2 AG\left\{\sigma^2\left[K_L + \right.\right.$$

$$\left. + 1 + \frac{1}{2}(2-n)\beta\mathscr{F}\right](K_L + 1)\left[\frac{1}{8}(2-n)\beta\mathscr{F}\left(X_{\ell.e.} + \frac{2}{5}\right) + \right.$$

$$\left. + \frac{2}{3}(1+K)\left(X_{\ell.e.} + \frac{3}{8}\right)\right] + \frac{1}{2}(2-n)\sigma^2\beta\mathscr{F}\left[K_L + 1 + \right.$$

$$\left. + \frac{1}{2}(2-n)\beta\mathscr{F}\right]\left[\frac{1}{24}(2-n)\beta\mathscr{F}\left(X_{\ell.e.} + \frac{8}{15}\right) + \frac{1}{6}(1+K)\left(X_{\ell.e.} + \frac{1}{2}\right)\right] -$$

$$- \frac{1}{2}(K_L + 1)\left(X_{\ell.e.} + \frac{1}{3}\right)\sigma\left[\frac{1}{2}(2-n)\sigma\beta\mathscr{F}K + \frac{1}{2}(1+n)\sigma^2\beta^2 AF + \right.$$

$$\left. + 2\sigma C + \frac{1}{8}K_{Lh}\right] + \left(\frac{b\omega}{V}\right)^2\left[\frac{1}{24}(2-n)\beta\mathscr{F}\left(X_{\ell.e.} + \frac{8}{15}\right) + \right.$$

$$\left.\left. + \frac{1}{6}(K_L + 1)\left(X_{\ell.e.} + \frac{1}{3}\right) + \frac{1}{6}(1+K)\left(X_{\ell.e.} + \frac{1}{2}\right)\right]\right\}$$

$$A_{1h} = -\left(\frac{\omega}{\omega_{na}}\right)^2\left(\frac{mb^2}{I_a}\right)X_a + \frac{1}{8}\beta F\left(\frac{a}{b}\right)\left(\frac{\rho b^4}{I_a}\right)\left(\frac{V}{b\omega_{na}}\right)^2\left[(2-n)\sigma v_{hr} + \right.$$

$$\left. + 2\sigma^4 n\beta A\frac{\mathscr{B}}{H}\right] + \left(\frac{\rho b^4}{I_a}\right)\left(\frac{V}{b\omega_{na}}\right)^2\left(\frac{V}{b\omega}\right)^2\sigma AG\left\{2\sigma^3\left[K_L + 1 + \right.\right.$$

$$\left. + \frac{1}{2}(2-n)\beta\mathscr{F}\right]\left[\frac{1}{2}(1+n)(K_L + 1)\sigma^2\beta^2 AF\left(X_{\ell.e.} + \frac{1}{3}\right) - \right.$$

$$\left. - \frac{1}{8}(2-n)\beta\mathscr{F}K_{Lh}\left(X_{\ell.e.} + \frac{1}{3}\right)\right] - 2\sigma\left(\frac{b\omega}{V}\right)^2\left\{\sigma\left[K_L + 1 + \right.\right.$$

$$\left. + \frac{1}{2}(2-n)\beta\mathscr{F}\right]\left[\frac{2}{3}(K_L + 1)\left(X_{\ell.e.} + \frac{3}{8}\right) + \frac{1}{12}(2-n)\beta\mathscr{F}\left(X_{\ell.e.} + \frac{1}{2}\right)\right] +$$

$$\left. + \frac{1}{4}K_{Lh}\left(X_{\ell.e.} + \frac{1}{3}\right) - \frac{1}{2}\sigma(K_L + 1)\left(X_{\ell.e.} + \frac{1}{3}\right)\left[\frac{1}{2}(2-n)\beta\mathscr{F} + 2\right]\right\} -$$

$$\left. - \frac{1}{3}\left(\frac{b\omega}{V}\right)^4\left(X_{\ell.e.} + \frac{1}{2}\right)\right\}$$

$$B_{1h} = \frac{1}{8}\,\beta F \left(\frac{a}{b}\right)\left(\frac{\rho b^4}{I_a}\right)\left(\frac{V}{b\omega_{na}}\right)^2 \left[(2-n)\sigma v_{hi} + (2-n)\sigma^2 A\left(\frac{b\omega}{V}\right)\right] +$$

$$+ 2\left(\frac{\rho b^4}{I_a}\right)\left(\frac{V}{b\omega_{na}}\right)^2 \left(\frac{V}{b\omega}\right)\sigma^2 AG \left\{\sigma^2(K_L+1)\left[K_L+1+\right.\right.$$

$$+ \frac{1}{2}(2-n)\beta\mathcal{F}\bigg]\left[\frac{1}{3}(2-n)\left(X_{\ell.e.}+\frac{3}{8}\right)\beta\mathcal{F} + X_{\ell.e.}+\frac{1}{3}\right] +$$

$$+ \frac{1}{24}\sigma^2(2-n)^2\beta^2\mathcal{F}^2\left(X_{\ell.e.}+\frac{1}{2}\right)\left[K_L+1+\frac{1}{2}(2-n)\beta\mathcal{F}\right] -$$

$$- \frac{1}{2}\sigma(K_L+1)\left(X_{\ell.e.}+\frac{1}{3}\right)\left[(1+n)\sigma^2\beta^2 AF + \frac{1}{2}K_{Lh}\right] +$$

$$+ \left(\frac{b\omega}{V}\right)^2\left[\frac{1}{12}(2-n)\left(X_{\ell.e.}+\frac{1}{2}\right)\beta\mathcal{F} + \frac{1}{2}(K_L+1)\left(X_{\ell.e.}+\frac{1}{3}\right)\right]\bigg\}$$

$$A_{2a} = -X_{\ell.e.} - \left(\frac{\omega}{\omega_{nh}}\right)^2(X_a - X_{\ell.e.}) + \left(\frac{\rho b^2}{m}\right)\left(\frac{V}{b\omega_{nh}}\right)^2\left(\frac{V}{b\omega}\right)^2 \sigma AG \times$$

$$\times \left\{2\sigma^3\left[K_L+1+\frac{1}{2}(2-n)\beta\mathcal{F}\right]\left\{(K_L+1)\left[\frac{1}{3}(2-n)\sigma\beta\mathcal{F}K+\right.\right.\right.$$

$$+ \frac{1}{3}(1+n)\sigma^2\beta^2 AF + \sigma K - \frac{1}{8}K_{Lh}\bigg] + \frac{1}{2}(2-n)\beta\mathcal{F}\left[\frac{1}{12}(2-n)\sigma\beta\mathcal{F}K+\right.$$

$$+ \frac{1}{12}(1+n)\sigma^2\beta^2 AF - \frac{3}{16}K_{Lh}\bigg]\bigg\} - 2\sigma\left(\frac{b\omega}{V}\right)^2\left\{\sigma\left[K_L+1+\right.\right.$$

$$+ \frac{1}{2}(2-n)\beta\mathcal{F}\right]\left[\frac{1}{4}(K_L+1) + \frac{1}{24}(2-n)\beta\mathcal{F}\right] + \frac{3}{16}K_{Lh} -$$

$$- \frac{1}{2}\sigma(K_L+1)\left[\frac{1}{6}(2-n)\beta\mathcal{F} + 1 + K\right] - \frac{1}{12}(2-n)\sigma\beta\mathcal{F}K -$$

$$- \frac{1}{12}(1+n)\sigma^2\beta^2 AF\right\} - \frac{1}{6}\left(\frac{b\omega}{V}\right)^4\right\}$$

$$B_{2a} = 2 \left(\frac{\rho b^2}{m}\right) \left(\frac{V}{b\omega_{nh}}\right)^2 \left(\frac{V}{b\omega}\right) \sigma^2 AG \left\{ \sigma^2 (K_L + 1)\left[K_L + 1 + \right.\right.$$

$$\left. + \frac{1}{2}(2 - n)\beta\mathcal{F}\right]\left[\frac{1}{8}(2 - n)\beta\mathcal{F} + \frac{2}{3}(1 + K)\right] + \frac{1}{2}\sigma^2 (2 - n)\beta\mathcal{F}\left[K_L + 1 + \right.$$

$$\left. + \frac{1}{2}(2 - n)\beta\mathcal{F}\right]\left[\frac{1}{24}(2 - n)\beta\mathcal{F} + \frac{1}{6}(1 + K)\right] - \frac{1}{2}\sigma(K_L + 1) \times$$

$$\times \left[\frac{1}{2}(2 - n)\sigma\beta\mathcal{F}K + \frac{1}{2}(1 + n)\sigma^2\beta AF + 2\sigma K + \frac{1}{8}K_{Lh}\right] +$$

$$\left. + \left(\frac{b\omega}{V}\right)^2\left[\frac{1}{24}(2 - n)\beta\mathcal{F} + \frac{1}{6}(K_L + 1) + \frac{1}{6}(1 + K)\right]\right\} - 2\zeta_h\left(\frac{\omega}{\omega_{nh}}\right)X_{\ell.e.}$$

$$A_{2h} = 1 - \left(\frac{\omega}{\omega_{nh}}\right)^2 + \left(\frac{\rho b^2}{m}\right) \left(\frac{V}{b\omega_{nh}}\right)^2 \left(\frac{V}{b\omega}\right)^2 \sigma AG \left\{ 2\sigma^3\left[K_L + 1 + \right.\right.$$

$$\left. + \frac{1}{2}(2 - n)\beta\mathcal{F}\right]\left[\frac{1}{2}(1 + n)(K_L + 1)\sigma^2\beta^2 AF - \frac{1}{8}(2 - n)\beta\mathcal{F}K_{Lh}\right] -$$

$$- 2\sigma \left(\frac{b\omega}{V}\right)^2 \left\{ \sigma\left[K_L + 1 + \frac{1}{2}(2 - n)\beta\mathcal{F}\right]\left[\frac{2}{3}(K_L + 1) + \frac{1}{12}(2 - n)\beta\mathcal{F}\right] + \right.$$

$$\left. + \frac{1}{4}K_{Lh} - \frac{1}{2}\sigma(K_L + 1)\left[2 + \frac{1}{2}(2 - n)\beta\mathcal{F}\right]\right\} - \frac{1}{3}\left(\frac{b\omega}{V}\right)^4 \right\}$$

$$B_{2h} = 2\zeta_h\left(\frac{\omega}{\omega_{nh}}\right) + 2 \left(\frac{\rho b^2}{m}\right) \left(\frac{V}{b\omega_{nh}}\right)^2 \left(\frac{V}{b\omega}\right) \sigma^2 AG \left\{ \sigma^2 (K_L + 1)\left[K_L + 1 + \right.\right.$$

$$\left. + \frac{1}{2}(2 - n)\beta\mathcal{F}\right]\left[\frac{1}{3}(2 - n)\beta\mathcal{F} + 1\right] + \frac{1}{24}\sigma^2(2 - n)^2\beta^2\mathcal{F}^2\left[K_L + 1 + \right.$$

$$\left. + \frac{1}{2}(2 - n)\beta\mathcal{F}\right] - \frac{1}{2}\sigma(K_L + 1)\left[(1 + n)\sigma^2\beta^2 AF + \frac{1}{2}K_{Lh}\right] +$$

$$\left. + \left(\frac{b\omega}{V}\right)^2\left[\frac{1}{12}(2 - n)\beta\mathcal{F} + \frac{1}{2}(K_L + 1)\right]\right\}$$

In these equations, the quantities not already defined are

$$K = 1 - \frac{2K_D W_s}{W - 2W_s}$$

24

$$G = 1 \left/ \left\{ 1 + \left(\frac{\sigma V}{b\omega}\right)^2 \left[K_L + 1 + \frac{1}{2}(2 - n)\beta \mathcal{J} \right]^2 \right\} \right.$$

$$v_o = V \left[v_{hr} + iv_{hi} \right] \frac{h_o}{b} + V \left[v_{ar} + iv_{ar} \right] a_o$$

and

$$v_{hr} = -\sigma^2 AG \left\{ 1 - K_L + \sigma \left(\frac{V}{b\omega}\right)^2 \left[K_L + 1 + \right. \right.$$
$$\left. \left. + \frac{1}{2}(2 - n)\beta \mathcal{J} \right] \left[(1 + n)\sigma^2 \beta^2 AF + \frac{1}{2} K_{Lh} \right] \right\}$$

$$v_{hi} = -\sigma AG \left(\frac{b\omega}{V}\right) \left\{ 1 + \sigma^2 \left[K_L + 1 + \frac{1}{2}(2 - n)\beta \mathcal{J} \right] \left[\frac{1}{2}(2 - n)\beta \mathcal{J} \right] \left(\frac{V}{b\omega}\right)^2 - \right.$$
$$\left. - \sigma \left[(1 + n)\sigma^2 \beta^2 AF + \frac{1}{2} K_{Lh} \right] \left(\frac{V}{b\omega}\right)^2 \right\}$$

$$v_{ar} = -\sigma^2 AG \left\{ K + \frac{2}{3} - \frac{1}{3} K_L + \sigma \left(\frac{V}{b\omega}\right)^2 \left[K_L + 1 + \right. \right.$$
$$\left. + \frac{1}{2}(2 - n)\beta \mathcal{J} \right] \left[\frac{1}{2}(2 - n)\sigma\beta \mathcal{J} K + \frac{1}{2}(1 + n)\sigma^2 \beta^2 AF + \right.$$
$$\left. \left. + 2\sigma K + \frac{1}{8} K_{Lh} \right] \right\}$$

$$v_{ai} = -\sigma AG \left(\frac{b\omega}{V}\right) \left\{ \frac{1}{3} + \sigma^2 \left[K_L + 1 + \frac{1}{2}(2 - n)\beta \mathcal{J} \right] \left[\frac{1}{6}(2 - n)\beta \mathcal{J} + \right. \right.$$
$$\left. + 1 + K \right] \left(\frac{V}{b\omega}\right)^2 - \sigma \left[\frac{1}{2}(2 - n)\sigma\beta \mathcal{J} K + \frac{1}{2}(1 + n)\sigma^2 \beta^2 AF + \right.$$
$$\left. \left. + 2\sigma K + \frac{1}{8} K_{Lh} \right] \left(\frac{V}{b\omega}\right)^2 \right\}$$

By eliminating a_o and h_o/b, the two equations to be solved simultaneously for V and ω are:

"Real" Equation $\quad A_{1a}A_{2h} + B_{1h}B_{2a} - B_{1a}B_{2h} - A_{1h}A_{2a} = 0 \qquad$ (A3)

"Imaginary" Equation $\quad A_{1a}B_{2h} + A_{2h}B_{1a} - A_{1h}B_{2a} - A_{2a}B_{1h} = 0 \quad$ (A4)

25

The solutions of Eqs. (A3) and (A4) are the critical velocity V and the critical frequency ω. Using these values of V and ω in Eq. (A1) allows the ratio $a_o/(h_o/b)$ to be calculated:

$$\frac{a_o}{(h_o/b)} = -\left(\frac{A_{1h} + iB_{1h}}{A_{1a} + iB_{1h}}\right) \tag{A5}$$

The translational amplitude of the elastic axis, h_{eo}, is related to h_o and a_o by $h_{eo} = h_o - bX_{l.e.}a_o$. Thus,

$$\frac{a_o}{(h_{eo}/b)} = \frac{1}{\dfrac{(h_o/b)}{a_o} - X_{l.e.}} \tag{A6}$$

Equation (A6) gives the ratio of the pitching to translational amplitude and the phase angle between them. This allows the mode of vibration to be determined (e.g., mostly pitch, mostly translation, or a combination).

There are two special cases that need to be treated separately:

(1) The torsion spring is "locked" (either K_h or ω_{nh} is infinite). For this case, the torsion equation need not be satisfied and $a_o = 0$. Thus, the equations to be solved are

$A_{2h} = 0$

$B_{2h} = 0$

(2) The translation spring is "locked" (either K_h or ω_{nh} is infinite). For this case, the translation equation need not be satisfied and $h_o = X_{l.e.}ba_o$. Thus, the equations to be solved are

$A_{1a} + X_{l.e.}A_{1h} = 0$

$B_{1a} + X_{l.e.}B_{1h} = 0$

The two natural modes of free vibration can be obtained from Eq. (A3) by setting $B_{1a} = B_{2a} = B_{1h} = B_{2h} = 0$ (i.e., neglecting damping) and letting $V = 0$. The results can be put in the form of

$$1 - B\left(\frac{\omega}{\omega_{na}}\right)^2 + E\left(\frac{\omega}{\omega_{na}}\right)^4\left(\frac{\omega_{na}}{\omega_{nh}}\right)^2 = 0 \tag{A7}$$

which can be solved by the quadratic equation for the two ω's identifying the natural modes. In Eq. (A7), B and E are

$$B = 1 - 2\left(\frac{mb^2}{I_a}\right)X_a X_{\ell.e.} + \frac{\rho b^4}{I_a}\left[\frac{1}{6}\left(X_{\ell.e.} + \frac{8}{15}\right) + \right.$$

$$\left. + \frac{1}{3}X_{\ell.e.}\left(X_{\ell.e.} + \frac{1}{2}\right)\right]\sigma A + \left(\frac{\omega_{na}}{\omega_{nh}}\right)^2\left[1 + \frac{1}{3}\sigma A\left(\frac{\rho b^2}{m}\right)\right]$$

$$E = \left\{1 - \left(\frac{mb^2}{I_a}\right)X_a X_{\ell.e.} + \sigma A\left(\frac{\rho b^4}{I_a}\right)\left[\frac{1}{6}\left(X_{\ell.e.} + \frac{8}{15}\right)\right]\right\}\left[1 + \right.$$

$$\left. + \frac{1}{3}\sigma A\left(\frac{\rho b^2}{m}\right)\right] - \left[X_a - X_{\ell.e.} + \frac{1}{6}\sigma A\left(\frac{\rho b^2}{m}\right)\right]\left[\left(\frac{mb^2}{I_a}\right)X_a + \right.$$

$$\left. + \frac{1}{3}\sigma A\left(\frac{\rho b^2}{I_a}\right)\left(X_{\ell.e.} + \frac{1}{2}\right)\right]$$

In B and E, the quantities involving "ρ" are the virtual mass effects of the fluid. When $\rho = 0$, the natural modes in a vacuum are obtained.

APPENDIX B. COMPUTER DOCUMENTATION

Equations (18) and (19) of Section, Analysis are solved numerically by a digital computer routine; in addition, certain other information is computed and printed out. The program is written in the FORTRAN IV language, and a complete listing is presented as part of this appendix.

All information to and from the program utilizes input and output tape units, and, thus, the logical tape unit numbers __must__ be defined by the user for each particular computer installation. The definition is given in the first two executable statements in the main program, where N is the logical input unit number and M is the logical output unit number; for example, in the CDC-3600 used by SwRI, N = 60 and M = 61.

Several optional kinds of input are available for the program. Unless otherwise specified in the input by the method described below, the physical properties of the flowing liquid are assumed to be those of standard air: $\rho = 4.34 \times 10^{-5}$ lb/in^3 and $\nu = 2.34 \times 10^{-2}$ in^2/sec. The inertia properties of the plate are specified by giving as input any two of K_h, ω_{nh}, and m for the translation mode alone and any two of K_α, $\omega_{n\alpha}$ and I_α for the pitch mode. The damping properties are specified by giving as input ζ_h or C_h and ζ_α or C_α. Finally, if steady state pressure drops are to be calculated, both K_o and L must be given as input.

Instructions for Input

A set of input data consists of three or four cards, depending on the options used. The format for the first two data cards is eight "E" fields of ten columns each (8E10.3). The remaining card(s) have a format of one "I" field of two columns followed by an eight column "E" field; this pair of fields is repeated eight times [8(I2, E8.0)].

The following parameters __must__ be given as input in the units shown: a (in.); b (in.); H (in.); W (in.); W_s (in.); X_α (no dimensions); $H\ell._e.$ (no dimensions); V_{max} (in/sec); ΔV (in/sec); test (no dimensions); XNO (no dimensions); any two of K_α (in-lb), I_α (lb-in), $\omega_{n\alpha}$ (rad/sec); any two of K_h (lb/in), m (lb/in), ω_{nh} (rad/sec); either C_h (lb-sec/in) or ζ_h (no dimensions); and either C_α (in-lb/sec) or ζ_α (no dimensions). The following parameters __may__ be given when desired: K_o (no dimensions); L (in.); K_D (no dimensions); ρ (lb/in^3); and ν (in^2/sec).

The input cards are to be punched as described in the following instructions:

29

1st Card

Card Columns	Data
1-10	plate thickness, a
11-20	plate length, b
21-30	channel height, H
31-40	channel width, W
41-50	width of the slots, W_s
51-60	nondimensional center-of-mass location, X_a
61-70	nondimensional location of plate leading edge, $X_{l.e.}$
71-80	maximum velocity considered, V_{max}

2nd Card

1-10	velocity increment, ΔV
11-20	solution convergence interval, TEST
21-30	number of parameters, XNO, to be entered on cards 3 and 4

3rd Card and 4th Card

Entered on these cards are the values of any of the following parameters to be used, with their identifying number:

1	K_a
2	I_a
3	ω_{na}
4	K_h
5	m
6	ω_{nh}
7	C_h
8	ζ_h
9	C_a
10	ζ_a
11	K_o
12	L
13	K_D
14	ρ
15	ν

Unless specified otherwise, the values of K_D, ρ, and ν are fixed as 0.6, 4.34×10^{-5} lb/in^3, and 1.13×10^{-6} in^2/sec, but they may be redefined as a group to any values desired by entering them as input

parameters. The use of K_0 and L is also optional as a group but if they are undefined as a group, the steady-state pressure drops ($P_0 - P_1$ and $P_1 - P_4$) will not be computed.

The parameters and their identifying numbers may be entered in any order; the format for each parameter with its identification is: two column "I" field for the identifying number (right justified) followed by an eight column "E" field for the parameter. Up to eight parameters can be given on each card, but the total number given on both cards must equal XNO. For example, if $\omega_{na} = 68.01$, $\omega_{nh} = 54.51$, $I_a = 0.0362$, $m = 0.117$, $\zeta_h = 0.0005$, and $\zeta_a = 0.0005$ are the only parameters of this group needed, then card 3 would be filled in as

Card Column	Data
2	3
3-10	68.01
12	6
13-20	54.51
22	2
23-30	0.0362
32	5
33-40	0.117
42	8
43-50	0.0005
51-52	10
53-60	0.0005

For this example, card columns 61 through 80 are blank, card number 4 is not needed and XNO = 6 is entered on card number 2 in columns 21 through 30.

Instructions for V_{max}, ΔV, and TEST

The control parameters V_{max}, ΔV, and TEST are set by the user. V_{max} is the maximum velocity to be considered in the search for a critical velocity; it should be determined by the user's judgement. If no solution is found for $V \leq V_{max}$, the calculations stop and "no solution" is indicated in the printout. ΔV is the increment used to stepup the trial values of V; for example, if no solution has yet been found below, say, $V = V_1$, then the program will next check for a solution in the range $V = V_1$ to

$V = V_1 + \Delta V$ as long as $V_1 + \Delta V \leq V_{max}$. TEST essentially sets the limit on the accuracy with which the equations are solved for V and ω; it is the width of the interval enclosing the "true" solution and the indicated numerical solution for both V and ω.

For faster computing times, ΔV should be picked as large as possible. However, difficulties may sometimes arise if such a large value of ΔV is used that two or more solutions are enclosed within one ΔV. In this case, the program may miss both solutions and continue to increment V. The reason for this is that the method of solution is to find the value of ω, if any, which satisfies the "real" equation for the trial value of V and then to determine the sign of the "imaginary" equation for this V and ω. This sign is then compared to the sign of the imaginary equation for $V + \Delta V$ and the ω satisfying the real equation for $V + \Delta V$. Thus two changes in sign in one ΔV interval will not be found by the computer routine. It is recommended that, at the beginning of any new set of runs, the optimum value of ΔV be found by trying a series of successively larger ΔV's.

Loss Coefficient, K_L

The loss coefficient for the channel contraction at Station 2 is automatically computed and no input is needed. The calculation has been accomplished by adapting the loss coefficients given in ref. 9 for contractions in parallel circular pipes to the case of narrow channel flow, on the basis of equal areas of contraction. Thus, K_L for any reduction (any σ) is interpolated from the following table, which is contained in the program as part of its data:

$\sigma^{-1/2}$	K_L
1.0	0.00
0.8	0.13
0.6	0.28
0.4	0.38
0.2	0.45
0.0	0.50

Also, since the derivative dK_L/dh equals $-(1/2)\sigma^{1/2}(dK_L/d\sigma^{-1/2})$, the rate of change of K_L as the plate translates is computed by numerical differentiation of the tabular values.

32

Special Cases of Input

There are two special cases sometimes encountered. The first is that of a rigid torsion spring (no pitching degree-of-freedom) in which either K_α or $\omega_{n\alpha}$ may be considered infinite. The second is that of a rigid translation degree-of-freedom) in which either K_h or ω_{nh} may be considered infinite. Either of these special cases can be treated merely by using input values of K_α or $\omega_{n\alpha}$ greater than 10^9 for the no-pitch condition, or K_h or ω_{nh} greater than 10^9 for the no-translation condition.

Program Accuracy and Limitations

The method of solution used in the program is one of searching for a change of sign until the solution is enclosed within a ΔV interval and then successively halving the interval until it is less than the value of TEST. The limits of the searching for the critical velocity and frequency are

$$0 \leq V \leq V_{max} \qquad \text{(in/sec)}$$

$$1 \leq \omega \leq 10\,\omega_0 \qquad \text{(rad/sec)}$$

V_{max}, ΔV, and TEST are input and ω_0 is the original estimate (equal to the smaller of $\omega_{n\alpha}$ or ω_{nh}) or the solution of ω from the "real" equation for the preceding value of V. The step size used is ΔV for velocity and, essentially, 1.2 times the preceding trial value for ω.

For the calculations performed to obtain the results given in this report, values of ΔV equal to 100 in/sec, V_{max} equal to 2500 in/sec, and TEST equal to 0.001 were found to be adequate. During test runs, the variation in the indicated solutions for V and ω for any ΔV in the range from 2 to 100 in/sec was less than 0.4 percent, while even less variation was found when TEST was changed for 0.001 to 0.000001. Running times were about six sec per case.

No provisions are included for running more than one set of input at a time; that, each change in any of the input parameters requires a separate reloading.

Computer Symbol List

In order to facilitate program changes by the user, a correspondence list of the symbols used in the program is given below. The quantities on the left are the FORTRAN alphanumeric symbols used in the computer program to denote the corresponding item on the right, used in the analysis or to identify computer operations.

A	-	a
A1A	-	A_{1a}
A2A	-	A_{2a}
A1H	-	A_{1h}
A2H	-	A_{2h}
B	-	b
B1A	-	B_{1a}
B2A	-	B_{2a}
B1H	-	B_{1h}
B2H	-	B_{2h}
BETA	-	β
CA	-	C_a
CAPA	-	A
CAPF	-	F
CAPH	-	H
CAPK	-	K_o
CAPL	-	L
CAPV	-	V
CD	-	K_D
CH	-	C_h
CL	-	K_L
CL1(I)	-	K_{Li} (the entries in the table of K_L vs $\sigma^{-1/2}$)
CLH	-	K_{Lh}
DELTAV	-	ΔV [the increment of V used in searching for roots of Eq. (A1) and (A2)]
DP1	-	$P_1 - P_4$
DP2	-	$P_0 - P_1$
M	-	Output Tape
N	-	Input Tape
OM	-	ω
OMEG	-	Estimated ω used as first guess
OMEGNA	-	ω_{na}
OMEGNH	-	ω_{nh}
RENO	-	N_{Re}
RHO	-	ρ
SCRIPD	-	$\mathscr{D}$
SCRIPF	-	$\mathscr{F}$
SIGMA	-	σ
SIGMA(I)	-	$(\sigma^{-1/2})_i$
VAI	-	v_{ai}
VAR	-	v_{ar}
VHI	-	v_{hi}
VHR	-	v_{hr}
VMAX	-	V_{max} (upper limit on V in searching for roots)
W	-	W
WS	-	W_s
XALPHA	-	X_a

XIA	-	I_α
XKH	-	K_h
XLE	-	$X_{\ell.e.}$
XM	-	m
XN	-	n
XNU	-	ν
X8	-	B
X9	-	E
Z	-	"Fluid Acceleration" switch
ZETAA	-	ζ_α
ZETAH	-	ζ_h
Z0, Z1	-	Residual of Real Equation
Z2, Z3	-	Residual of Imaginary Equation

Flow Charts, Computer Listing, and Sample Output

The following pages (35 through 46) give flow charts describing the program logic and operations. A complete listing of each card in the deck (as run on the CDC-3600 used by SwRI) then follows on pages 47 through 55. Then on page 56 the form of the output for a typical run is given. The first four lines of the output list the input parameters with their units. The next two lines give the natural frequencies of the normal modes both with virtual air mass considered and also not considered. The next line of output lists the values of ρ, ν, and K_D used in the program. The next four lines of output give the critical velocity (V) in the unobstructed main channel, the flutter frequency (ω), the nondimensional ratio of the pitch amplitude to the translation amplitude ($\alpha_o b / h_{eo}$), and the phase angle between the pitch and the acceleration. If no solution is found, it is so indicated. The next four lines list the same four quantities for the quasi-steady case ($\dot{\alpha} = \ddot{\alpha} = \dot{h} = \ddot{h} = 0$ in deriving flow velocities and pressures). The last two lines give $P_0 - P_1$ and $P_1 - P_4$ whenever K_o and L are given as input; in the sample case shown, K_o and L are not given (which is indicated by their being equal to zero in the input printout), so no pressure drops are given.

PROGRAM FLUTTER

START

```
V ← 0
WITCH 1 ← 0
WITCH 2 ← 0
$C_D$ ← .6
$\rho$ ← 4.34 x $10^{-5}$
$\nu$ ← 2.34 x $10^{-2}$
```

READ a, b, H, W,
W_s, X_α, X_{Ae}, V_{max}
ΔV, TEST, XNO

NO ← XNO

READ III_j, VALUE_j
j = 1, NO

25
```
i ← $\text{III}_j$
$\text{VLU}_i$ ← $\text{VALUE}_j$
j = 1, NO
```

```
$K_\alpha$ ← $\text{VLU}_1$
$I_\alpha$ ← $\text{VLU}_2$
$\omega_{n\alpha}$ ← $\text{VLU}_3$
$K_h$ ← $\text{VLU}_4$
m ← $\text{VLU}_5$
$\omega_{nh}$ ← $\text{VLU}_6$
$C_h$ ← $\text{VLU}_7$
$\zeta_h$ ← $\text{VLU}_8$
$C_\alpha$ ← $\text{VLU}_9$
$\zeta_\alpha$ ← $\text{VLU}_{10}$
```

(1)

(1)

i ← 0

i ← i + 1

35   30

III_j - 12

```
+
$C_D$ ← $\text{VLU}_{13}$
$\rho$ ← $\text{VLU}_{14}$
$\nu$ ← $\text{VLU}_{15}$
```

```
o
$K_0$ ← $\text{VLU}_{11}$
L ← $\text{VLU}_{12}$
WITCH 2 ← 1
```

40

i > NO   No

Yes

(2)

36

2

$j \leftarrow 0$

$j \leftarrow j + 1$

$i \leftarrow 0$

$i \leftarrow i + 1$

III_{i-j} o   ±

46    $i > NO$ No

Yes

$j = ?$

1    $K_\alpha \leftarrow I_\alpha \omega_{n\alpha}^2 (W - 2W_s)$

2    $I_\alpha \leftarrow \dfrac{K_\alpha}{(W - 2W_s)\omega_{n\alpha}^2}$

3    $\omega_{n\alpha} \leftarrow \sqrt{\dfrac{K_\alpha}{I_\alpha (W - 2W_s)}}$

4    $K_h \leftarrow m(W - 2W_s)\omega_{nh}^2$

5    $m \leftarrow \dfrac{K_h}{(W - 2W_s)\omega_{nh}^2}$

6    $\omega_{nh} \leftarrow \sqrt{\dfrac{K_n}{m(W - 2W_s)}}$

7    $C_h \leftarrow 2m\omega_{nh}(W - 2W)\zeta_h$

8    $\zeta_h \leftarrow \dfrac{C_h}{2m\omega_{nh}(W - 2W_s)}$

9    $C_\alpha \leftarrow 2I_\alpha \omega_{n\alpha}(W - 2W_s)\zeta_\alpha$

10    $\zeta_\alpha \leftarrow \dfrac{C_\alpha}{2I_\alpha \omega_{n\alpha}(W - 2W_s)}$

48    $i > 10$ No

Yes

3

37

③

$K_h + \omega_{nh} > 10^9$ — Yes → 50 — WITCH 1 ← +1

No

$K_a + \omega_{na} > 10^9$ — Yes → 70 — WITCH 1 ← -1

No

72 — $\omega_{nh} - \omega_{na}$ — − → 73 — OMEG ← ω_{nh}

°+

74 — OMEG ← ω_{na}

75

$$\sigma \leftarrow \frac{H}{H - a}$$

$$D \leftarrow \frac{HW}{\frac{H}{2} + \sigma(W - W_s)}$$

$$\beta \leftarrow \frac{W - W_s}{W}$$

$$SIGMA\ 2 \leftarrow \frac{1}{\sqrt{\sigma}}$$

④

(4)

80

$C_L \leftarrow CL1$
$i \leftarrow 2$

o ← SIGMA 2 - 1 → +

100

ERROR EXIT

90

$i \leftarrow 0$

$i \leftarrow i + 1$

110

$C_L \leftarrow CL1_i$

o ← SIGMA 1_i - SIGMA 2 → +

No

$i > 6$ → Yes

120

$$C_L \leftarrow \frac{(CL1_i - CL1_{i-1})(SIGMA\ 2 - SIGMA\ 1_i)}{SIGMA\ 1_i - SIGMA\ 1_{i-1}} + CL1_i$$

130

$$C_{Lh} \leftarrow \frac{-.5\sqrt{\sigma}(CL1_i - CL1_{i-1})}{SIGMA\ 1_i - SIGMA_{i-1}}$$

WRITE
H, W, K_o, L
$a, b, X_{\ell.e.}, W_s, X_\alpha,$
$I_\alpha, K_\alpha, \omega_{na}, \zeta_\alpha,$
$m, K_h, \omega_{nh}, \zeta_h$

WITCH 1 → $\pm$

190

(6)

135 o

SAVER $\leftarrow \rho$
$\rho \leftarrow 0$

(5)

39

(6)

190

WRITE
$\omega_{01}, \omega_{02}, \omega_1, \omega_2$

$$\omega_{01} \leftarrow \frac{\omega_{01}}{6.28318}$$

$$\omega_{02} \leftarrow \frac{\omega_{02}}{6.28318}$$

$$\omega_1 \leftarrow \frac{\omega_1}{6.28318}$$

$$\omega_2 \leftarrow \frac{\omega_2}{6.28318}$$

WRITE
$\omega_{01}, \omega_{02}, \omega_1, \omega_2$
P, ν, C_D

$z = 1$

195

$V \leftarrow V + 2\Delta V$

$\omega \leftarrow$ OMEG

(8)

242

No $V > V_{max}$ Yes   (12)

196

SUBROUTINE
FREQ
Z 2

100

o ω −   ERROR EXIT

+

300

Z 2   o   (10)

+
−

(7)

41

42

Flowchart:

(11) → WITCH 1 (decision, + / -)

310

$$X1 \leftarrow A_{1h}^2 + B_{1h}^2$$
$$X2 \leftarrow A_{1h}B_{1\alpha} - A_{1\alpha}B_{1h}$$
$$X3 \leftarrow X1(X_{\ell.e.}) + A_{1\alpha}A_{1h} + B_{1\alpha}B_{1h}$$
$$RPATA \leftarrow \frac{X1}{\sqrt{X3^2 + X2^2}}$$
$$\theta_r \leftarrow \text{Arctan} \frac{-X2}{X3}$$
$$\theta_o \leftarrow 57.2958\ \theta_r$$

WRITE RPATA θ_r, θ_o

320 WITCH 2 (decision, + / $\bar{0}$)

330
$$\Delta P_1 \leftarrow .001295 \rho V^2 \left[(C_2 + 1)\sigma^2 - 1 + \sigma^2 \mathcal{F} \right]$$

WRITE ΔP_1

$$\mathcal{D} = \frac{2HW}{H+W}$$
$$N_{Re} = \frac{V\mathcal{D}}{\nu}$$

SUBROUTINE FRC FAC

$$\Delta P_2 \leftarrow .001295 \rho V^2 \left(K_o + \frac{F_o L}{\mathcal{D}} \right)$$

WRITE ΔP_2

360 EXIT ← 340 Z (decision, $\pm$) → $Z \leftarrow 0$ $V \leftarrow 0$ → (8)

44

SUBROUTINE FREQ

START

V = 0

Yes

No

180

$N_{Re} - \dfrac{V D \sigma}{\nu}$

SUBROUTINE
FRC FAC
F

$\mathcal{J} - \dfrac{Fb}{D}$

190

SUBROUTINE
EQNS
Z0, Z2

SAVE K — ω

Z0 = 0

Yes

300

RETURN

200

No

$\omega_1 - 1$

SUBROUTINE
EQNS
Z1, Z2

Z1 = 0

Yes

210

ω — ω_1

300

RETURN

No

245

SUBROUTINE
EQNS
Z0, Z2

240

$\omega_1 - \omega$
Z1 — Z0
ω — ω + .2ω

+

220

Z0(Z1)

0

Yes

ω ≤ 10 SAVE K

No

290

ω — 0

300

RETURN

230

$\omega_2 - \omega$

1

1

250

$\omega - \omega_1 + \dfrac{\omega_2 - \omega_1}{2}$

SUBROUTINE
EQNS
Z0, Z2

$\left| \dfrac{\omega_2 - \omega_1}{\omega} \right| \le$ TEST

Yes

300

RETURN

No

280

$\omega_2 - \omega$

−

260

Z0(Z1)

0

270

+

$\omega_1 - \omega$
Z1 — Z0

45

SUBROUTINE EQNS

START

Intermediate
Calculations

V = 0 — Yes

5
Calculate $A_{1\alpha}, B_{1\alpha}, A_{1h}, B_{1h}, A_{2\alpha}, B_{2\alpha}, A_{2h}, B_{2h}$
ZERO 1 $\leftarrow A_{1\alpha}A_{2h} + B_{1h}B_{2\alpha} - B_{1\alpha}B_{2h} - A_{1h}A_{2\alpha}$
ZERO 2 $\leftarrow A_{1\alpha}B_{2h} + A_{2h}B_{1\alpha} - A_{1h}B_{2\alpha} - A_{2\alpha}B_{1h}$

No

7
Calculate
A_{2h}, B_{2h}

WITCH 1

10
ZERO 1 $\leftarrow A_{2h}$
ZERO 2 $\leftarrow B_{2h}$

300
RETURN

o
+

20
Calculate
$v_{hr}, v_{hi}, v_{\alpha r}, v_{\alpha i}$
$A_{1\alpha}, B_{1\alpha}, A_{1h}, B_{1h}$

WITCH 1 — ±

30
ZERO 1 $\leftarrow A_{1\alpha} + X_{\ell.e.}A_{1\alpha}$
ZERO 2 $\leftarrow B_{1\alpha} + X_{\ell.e.}B_{1h}$

o

40
Calculate $A_{2\alpha}, B_{2\alpha}$
ZERO 1 $\leftarrow A_{1\alpha}A_{2h} + B_{1h}B_{2\alpha} - B_{1\alpha}B_{2h} - A_{1h}A_{2\alpha}$
ZERO 2 $\leftarrow A_{1\alpha}B_{2h} + A_{2h}B_{1\alpha} - A_{1h}B_{2\alpha} - A_{2\alpha}B_{1h}$
ZERO 2 $\leftarrow$ ZERO 2 $\left(\dfrac{bV}{\omega}\right)$

300
RETURN

46

SUBROUTINE FRC FAC

START

150
$n \leftarrow 1$
$F \leftarrow \dfrac{64}{N_{Re}}$

Yes $N_{Re} \leq 1828.57$

No

160
$N_{Re} < 6644.7$

170
$n \leftarrow 0$
$F \leftarrow .035$

Yes

No

180
$n \leftarrow .25$
$F \leftarrow \dfrac{.316}{(N_{Re})^n}$

RETURN

```
      PROGRAM FLUTTER
1100 FORMAT(8E10.3)
1110 FORMAT(8(I2,E8.0))
      DIMENSION SIGMA1(6),CL1(6)
      DIMENSION VALUE(15),VLU(15),III(15)
      COMMON A,A1A,A1H,B,B1A,B1H,BETA,CAPA,CAPF,CAPH,CD,CL,CLH,
     1       OMEGNA,OMEGNH,RHO,SCRIPD,SCRIPF,SIGMA,TEST,W,WITCH1,WS,
     2       XALPHA,XIA,XLE,XM,XN,XNU,Z,ZETAA,ZETAH
      DATA((SIGMA1(I),I=1,6)=1.,.8,.6,.4,.2,0.)
      DATA((CL1(I),I=1,6)=0.,.13,.28,.38,.45,.5)
      N=60
      M=61
      CAPV=0.0
      WITCH1=0.0
      WITCH2=0.0
      CD=.6
      RHO=4.34E-5
      XNU=2.34E-2
      READ(N,1100) A,B,CAPH,W,WS,XALPHA,XLE,VMAX,DELTAV,TEST,XNO
      NO=XNO
      READ(N,1110) (III(J),VALUE(J),J=1,NO)
      DO 25 J=1,NO
      I=III(J)
   25 VLU(I)=VALUE(J)
      XKA=VLU(1)
      XIA=VLU(2)
      OMEGNA=VLU(3)
      XKH=VLU(4)
      XM=VLU(5)
      OMEGNH=VLU(6)
      CH=VLU(7)
      ZETAH=VLU(8)
      CA=VLU(9)
      ZETAA=VLU(10)
      DO 40 I=1,NO
      IF(III(I)-12)40,30,35
   30 CAPK=VLU(11)
      CAPL=VLU(12)
      WITCH2=1.0
      GO TO 40
   35 CD=VLU(13)
      RHO=VLU(14)
      XNU=VLU(15)
   40 CONTINUE
   42 DO 48 J=1,10
      J=J
      DO 46 I=1,NO
      IF(III(I)-J)46,48,46
   46 CONTINUE
      GO TO (1,2,3,4,5,6,7,8,9,10),J
    1 XKA=XIA*OMEGNA**2*(W=2.*WS)
      GO TO 48
```

```
  2 XIA=XKA/((w-2.*wS)*OMEGNA**2)
    GO TO 48
  3 OMEGNA=(XKA/(XIA*(W-2.*wS)))**.5
    GO TO 48
  4 XKH=XM*(W-2.*WS)*OMEGNH**2
    GO TO 48
  5 XM=XKH/((W-2.*WS)*OMEGNH**2)
    GO TO 48
  6 OMEGNH=(XKH/(XM*(W-2.*WS)))**.5
    GO TO 48
  7 CH=2.*XM*OMEGNH*(W-2.*WS)*ZETAH
    GO TO 48
  8 ZETAH=CH/(2.*XM*OMEGNH*(W-2.*WS))
    GO TO 48
  9 CA=2.*XIA*OMEGNA*(W-2.*wS)*ZETAA
    GO TO 48
 10 ZETAA=CA/(2.*XIA*OMEGNA*(W-2.*WS))
 48 CONTINUE
    IF(XKH+OMEGNH-1.E9)60,60,50
 50 WITCH1=1.0
 60 IF(XKA+OMEGNA-1.E9)72,72,70
 70 WITCH1=-1.0
 72 IF(OMEGNH-OMEGNA)73,74,74
 73 OMEG=OMEGNH
    GO TO 75
 74 OMEG=OMEGNA
 75 CAPA=B/CAPH
    SIGMA=CAPH/(CAPH-A)
    SCRIPD=CAPH*-/(CAPH/2.+SIGMA*(w-wS))
    BETA=(w-WS)/-
    SIGMA2=1./SIGMA**.5
    IF(SIGMA2-1.0)90,80,100
 80 CL=CL1(1)
    I=2
    GO TO 130
 90 DO 100 I=1,6
    I=I
    IF(SIGMA1(I)-SIGMA2) 120,110,100
100 CONTINUE
    WRITE(M,1085)
    GO TO 360
110 CL=CL1(I)
    GO TO 130
120 CL=(CL1(I)-CL1(I-1))*(SIGMA2-SIGMA1(I))/(SIGMA1(I)-SIGMA1(I-1))
   1    +CL1(I)
130 CLH=-.5*SIGMA**.5*(CL1(I)-CL1(I-1))/(SIGMA1(I)-SIGMA1(I-1))
    WRITE(M,1005)
    WRITE(M,1010)
    WRITE(M,1012) CAPH,w,CAPK,CAPL
    WRITE(M,1015)
    WRITE(M,1020)
    WRITE(M,1022) A,B,XLE,WS,XALPHA
```

```
      WRITE(M,1025)
      WRITE(M,1027) XIA,XKA,OMEGMA,ZETAA
      WRITE(M,1030)
      WRITE(M,1031) XM,XKM,OMEGNM,ZETAM
      WRITE(M,1032)
      WRITE(M,1033)
      IF(WITCH1)190,135,190
  135 SAVER=RHO
      RHO=0.0
  140 X8=1.-2.*XM*B**2*XALPHA*XLE/XIA+RHO*B**4/XIA*(1./6.*(XLE+8./15.)
     1    +1./3.*XLE*(XLE+.5))*SIGMA*CAPA+(OMEGNA/OMEGNM)**2*
     2    (1.+1./3.*SIGMA*CAPA*RHO*B**2/XM)
      X9=(1.-XM*B**2*XALPHA*XLE/XIA+SIGMA*CAPA*RHO*B**4/XIA*
     1    (1./6.*(XLE+8./15.)))*(1.+1./3.*SIGMA*CAPA*RHO*B**2/XM)
     2    -(XALPHA-XLE+1./6.*SIGMA*CAPA*RHO*B**2/XM)*
     3    (XM*B**2*XALPHA/XIA+1./3.*SIGMA*CAPA*RHO*B**4/XIA*(XLE+.5))
      X10=X8**2-4.*X9*(OMEGNA/OMEGNM)**2
      IF(X10)100,150,150
  150 X10=X10**.5
      OMSQ1=(X8+X10)/(2.*X9/OMEGNM**2)
      OMSQ2=(X8-X10)/(2.*X9/OMEGNM**2)
      IF(OMSQ1)100,160,160
  160 OM1=OMSQ1**.5
      IF(OMSQ2)100,170,170
  170 OM2=OMSQ2**.5
      IF(RHO)190,180,190
  180 RHO=SAVER
      OM01=OM1
      OM02=OM2
      GO TO 140
  190 WRITE(M,1034) OM01,OM02,OM1,OM2
      OM01=OM01/6.28318
      OM02=OM02/6.28318
      OM1=OM1/6.28318
      OM2=OM2/6.28318
      WRITE(M,1035) OM01,OM02,OM1,OM2
      WRITE(M,1037)
      WRITE(M,1040)
      WRITE(M,1042) RHO,XNU,CL
      WRITE(M,1045)
      WRITE(M,1050)
      Z=1.0
  195 CAPV=CAPV+2.*DELTAV
      OM=OMEG
      IF(CAPV-VMAX)196,196,242
  196 CALL FREQ(Z2,CAPV,OM)
      IF(OM)100,195,197
  197 IF(Z2)198,300,196
  198 IF(CAPV-2.*DELTAV)200,199,200
  199 CAPV1=0.0
      OM=OMEG
      GO TO 202
```

51

```
200 CAPV1=CAPV-DELTAV
    OM=.5*OM
202 CALL FREQ(Z3,CAPV1,OM)
    IF(OM)100,195,205
205 IF(Z3)220,210,220
210 CAPV=CAPV1
    GO TO 300
220 IF(Z2*Z3)230,300,240
230 CAPV2=CAPV
    GO TO 250
240 CAPV1=CAPV
    Z3=Z2
    CAPV=CAPV+DELTAV
    IF(CAPV-VMAX)245,245,242
242 WRITE(M,1090) VMAX
    GO TO 360
245 OM=.9*OM
    CALL FREQ(Z2,CAPV,OM)
    IF(OM)100,195,220
250 CAPV=CAPV1+(CAPV2-CAPV1)/2.0
    OM=.9*OM
    CALL FREQ(Z2,CAPV,OM)
    IF(OM)100,195,255
255 IF(ABS((CAPV2-CAPV1)/CAPV)-TEST)300,300,260
260 IF(Z2*Z3) 280,300,270
270 CAPV1=CAPV
    Z3=Z2
    GO TO 250
280 CAPV2=CAPV
    GO TO 250
300 OMECYC=OM/6.28318
    WRITE(M,1055) CAPV,OM,OMECYC
    IF(WITCH1)320,310,320
310 X1=A1H**2+B1H**2
    X2=A1H*B1A-A1A*B1H
    X3=X1*XLE+A1A*A1H+B1A*B1H
    RPATA=X1/(X3**2+X2**2)*(X3**2+X2**2)**.5
    THETA=ATAN(-X2/X3)
    THETAD=57.2956*THETA
    WRITE(M,1060) RPATA
    WRITE(M,1065) THETA,THETAD
320 IF(WITCH2)340,340,330
330 DP1=.001295*RHO*CAPV**2*((CL+1.)*SIGMA**2-1.+SIGMA**2*SCRIPF)
    SCRIPD=2.*CAPH*W/(CAPH+W)
    RENO=CAPV*SCRIPD/XNU
    CALL FRCFAC(CAPF,XN,RENO)
    DP2=.001295*RHO*CAPV**2*(CAPK+CAPF*CAPL/SCRIPD)
    WRITE(M,1070) DP1
    WRITE(M,1075) DP2
340 IF(Z)350,360,350
350 WRITE(M,1080)
    Z=0.0
```

```
      CAPV=0.0
      GO TO 195
  360 STOP
 1005 FORMAT(1H1,55X,16HCHANNEL GEOMETRY)
 1010 FORMAT(120H0                   HEIGHT                              WIDTH
     1                 ENTRANCE LOSS FACTOR              LENGTH UPSTREAM )
 1012 FORMAT(10X,F7.3,3H IN,23X,F7.4,3H IN,24X,F7.3,22X,F7.3,3H IN)
 1015 FORMAT(1H0,55X,16HPLATE PARAMETERS)
 1020 FORMAT(120H0                  THICKNESS                             LENGTH
     1 ND L.E. DISTANCE      SLOTWIDTH                    ND E.A. DISTANCE)
 1022 FORMAT(11X,F7.4,3H IN,22X,F7.5,3H IN,7X,F7.4,10X,F7.5,3H IN,
     1      21X,F7.4)
 1025 FORMAT(129H0      MOM. INTERTIA/UNIT WIDTH              ALPHA SPRING CO
     1NST           ALPHA NATURAL FREC         ALPHA DAMPING RATIO
     2           )
 1027 FORMAT(10X,F7.4,6H LB-IN,19X,F7.2,6H IN-LB,18X,F7.2,8H RAD/SEC,
     119X,F8.5)
 1030 FORMAT(120H0               MASS/UNIT WIDTH                   H SPRING CONS
     1T                 H NATURAL FREG                 H DAMPING RATIO )
 1031 FORMAT(10X,F7.4,6H LB/IN,19X,F7.1,6H LB/IN,18X,F7.2,8H RAD/SEC,
     119X,F8.5)
 1032 FORMAT(1H0,53X,19HNATURAL FREQUENCIES)
 1033 FORMAT(120H0          NO VIRTUAL AIRMASS                  NO VIRTUAL AIRM
     1ASS            VIRTUAL AIRMASS             VIRTUAL AIRMASS )
 1034 FORMAT(8X,F7.2,8H RAD/SEC,16X,F7.2,8H RAD/SEC,16X,F7.2,8H RAD/SEC,
     1      16X,F7.2,8H RAD/SEC)
 1035 FORMAT(6X,F7.2,11H CYCLES/SEC,15X,F7.2,11H CYCLES/SEC,14X,F7.2,
     1      11H CYCLES/SEC,13X,F7.2,11H CYCLES/SEC)
 1037 FORMAT(1H0,53X,15HFLOW PARAMETERS)
 1040 FORMAT(120H0          FLUID DENSITY                   KINEMATIC VISCOS
     1ITY                 CROSSFLOW LOSS COEF                         )
 1042 FORMAT(6X,E10.2,9H LB/CU IN,13X,E10.2,10H SQ IN/SEC,19X,F7.3)
 1045 FORMAT(17H0           RESULTS)
 1050 FORMAT(44H0              FLUID ACCELERATION CONSIDERED)
 1055 FORMAT(1H0,19X,15HFLUTTER SPEED =E11.4,7H IN/SEC//20X19HFLUTTER FR
     1EQUENCY =F7.2,10H RAD/SEC =F7.2,11H CYCLES/SEC)
 1060 FORMAT(88H0                  RATIO OF PITCHING AMPLITUDE TO DIMEN
     1SIONLESS TRANSLATION AMPLITUDE =F9.4)
 1065 FORMAT(66H0                 PHASE ANGLE BETWEEN PITCHING AND TRA
     1NSLATION =F9.4,6H RAD =F9.3,4H DEG)
 1070 FORMAT(73H0                 PRESSURE DROP FROM JUST UPSTREAM TO
     1JUST DOWNSTREAM =F9.4,9H LB/SQ IN)
 1075 FORMAT(65H0                 PRESSURE DROP FROM OUTSIDE TO JUST U
     1PSTREAM =F9.4,9H LB/SQ IN)
 1080 FORMAT(48H0              FLUID ACCELERATION NOT CONSIDERED)
 1085 FORMAT(1H1,10X,11HINPUT ERROR)
 1090 FORMAT(1H0,19X,31HNO SOLUTION FOUND BELOW SPEED =E11.4,7H IN/SEC)
      END
```

```
      SUBROUTINE FREQ(Z2,CAPV,XK)
      COMMON A,A1A,A1H,B,B1A,B1H,BETA,CAPA,CAPF,CAPH,CD,CL,CLH,
     1        OMEGNA,OMEGNH,RHO,SCRIPD,SCRIPF,SIGMA,TEST,W,WITCH1,WS,
     2        XALPHA,XIA,XLE,XM,XN,XNU,Z,ZETAA,ZETAH
      IF(CAPV)180,190,180
180   RENU=CAPV*SCRIPD*SIGMA/XNU
      CALL FRCFAC(CAPF,XN,RENU)
      SCRIPF=CAPF*H/SCRIPD
190   CALL EQNS(Z0,Z2,XK,CAPV)
      SAVEK=XK
      IF(Z0)200,300,200
200   XK1=1.0
      CALL EQNS(Z1,Z2,XK1,CAPV)
      IF(Z1) 220,210,220
210   XK=XK1
      GO TO 300
220   IF(Z0*Z1)230,300,240
230   XK2=XK
      GO TO 250
240   XK1=XK
      Z1=Z0
      XK=XK+.2*XK
      IF(XK-10.*SAVEK)245,245,290
245   CALL EQNS(Z0,Z2,XK,CAPV)
      GO TO 220
250   XK=XK1+(XK2-XK1)/2.0
      CALL EQNS(Z0,Z2,XK,CAPV)
      IF(ABS((XK2-XK1)/XK)-TEST)300,300,260
260   IF(Z0*Z1) 280,300,270
270   XK1=XK
      Z1=Z0
      GO TO 250
280   XK2=XK
      GO TO 250
290   XK=0.0
300   RETURN
      END
```

```
      SUBROUTINE EGNS(ZERO1,ZERO2,OM,CAPV)
      COMMON A,A1A,A1H,B,B1A,B1H,BETA,CAPA,CAPF,CAPH,CD,CL,CLH,
     1       OMEGNA,OMEGNH,RHO,SCRIPD,SCRIPF,SIGMA,TEST,W,WITCH1,WS,
     2       XALPHA,XIA,XLE,XM,XN,XNU,Z,ZETAA,ZETAH
      X1=(2.-XN)*BETA*SCRIPF
      X2=(1.+XN)*SIGMA**2*BETA**2*CAPA*CAPF
      X3=XLE+1./3.
      X4=CL+1.+.5*X1
      X13=1./3.
      X16=1./6.
      X23=2./3.
      X112=1./12.
      X124=1./24.
      X815=8./15.
      IF(CAPV)7,5,7
    5 A1A=1.-(OM/OMEGNA)**2*(1.-XM*B**2*XALPHA*XLE/XIA)
     1    -X16*SIGMA*CAPA*RHO*B**4/XIA*(XLE+X815)*(OM/OMEGNA)**2
      B1A=2.*ZETAA*OM/OMEGNA
      A1H=-(OM/OMEGNA)**2*XM*B**2*XALPHA/XIA
     1    -X13*SIGMA*CAPA*RHO*B**4/XIA*(XLE+.5)*(OM/OMEGNA)**2
      B1H=0.0
      A2A=-XLE-(OM/OMEGNH)**2*(XALPHA-XLE)
     1    -X16*SIGMA*CAPA*RHO*B**2/XM*(OM/OMEGNH)**2
      B2A=-2.*ZETAH*OM*XLE/OMEGNH
      A2H=1.-(OM/OMEGNH)**2-X13*SIGMA*CAPA*RHO*B**2/XM*(OM/OMEGNH)**2
      B2H=2.*ZETAH*OM/OMEGNH
      ZERO1=A1A*A2H+B1H*B2A-B1A*B2H-A1H*A2A
      ZERO2=A1A*B2H+A2H*B1A-A1H*B2A-A2A*B1H
      GO TO 300
    7 CLA=-.5*CLH
      C=1.-2.*CD*WS/(W-2.*WS)
      G=1./(Z+(SIGMA*CAPV/(B*OM))**2*X4**2)
      A2H=1.-(OM/OMEGNH)**2+RHO/XM*(CAPV/OMEGNH)**2*(CAPV/(B*OM))**2
     1    *SIGMA*CAPA*G*(2.*SIGMA**3*X4*(.5*(CL+1.)*X2-.125*X1*CLH)
     2    -2.*Z*SIGMA*(B*OM/CAPV)**2*(SIGMA*X4*(X23*(CL+1.)+X112*X1)
     3    +.25*CLH-.5*SIGMA*(CL+1.)*(2.+.5*X1))-Z*X13*(B*OM/CAPV)**4)
      B2H=2.*ZETAH*OM/OMEGNH+2.*RHO/XM*(CAPV/OMEGNH)**2*CAPV/(B*OM)
     1    *Z*SIGMA**2*CAPA*G*(SIGMA**2*(CL+1.)*X4*(X13*X1+1.)
     2    +X124*SIGMA**2*X1**2*X4-.5*SIGMA*(CL+1.)*(X2+.5*CLH)
     3    +(B*OM/CAPV)**2*(X112*X1+.5*(CL+1.)))
      IF(WITCH1)10,20,20
   10 ZERO1=A2H
      ZERO2=B2H
      GO TO 300
   20 VHR=-SIGMA**2*CAPA*G*(Z*(1.-CL)+SIGMA*(CAPV/(B*OM))**2
     1    *X4*(X2+.5*CLH))
      VHI=-2*SIGMA*CAPA*G*B*OM/CAPV*(1.+SIGMA**2*X4*.5*X1*
     1    (CAPV/(B*OM))**2-SIGMA*(X2+.5*CLH)*(CAPV/(B*OM))**2)
      VAR=-SIGMA**2*CAPA*G*(Z*(C+X23-X13*CL)+SIGMA*(CAPV/(B*OM))**2
     1    *X4*(.5*X1*SIGMA*C+.5*X2+2.*SIGMA*C-.25*CLA))
      VAI=-Z*SIGMA*CAPA*G*B*OM/CAPV*(X13+SIGMA**2*X4*(X16*X1+1.+C)*
     1    (CAPV/(B*OM))**2-SIGMA*(.5*X1*SIGMA*C+.5*X2+2.*SIGMA*C
```

55

```
2      -.25*CLA)*(CAPV/(B*OM))**2)
   A1A=1.-(OM/OMEGNA)**2*(1.-XM*B**2*XALPHA*XLE/XIA)+
1      .125*BETA*CAPF*A*RHO*B/XIA*(CAPV/OMEGNA)**2*((2.-XN)*SIGMA*VAR
2      +(2.-XN)*SIGMA**3*CAPA*C*SIGMA**4*XM*BETA*CAPA*SCRIPL/CAPH)
3      +RHO/XIA*(CAPV/OMEGNA)**2*(CAPV/OM)**2*SIGMA*CAPA*G*
4      (2.*SIGMA**3*X4*((CL+1.)*(X13*X1*SIGMA*C*X3+.25*CLA*(XLE+.5)
5      +X13*X2*(XLE+.375)+SIGMA*C*X3)+.5*X1*(X112*X1*SIGMA*C*(XLE+.5)
6      +X112*X2*X3+.375*CLA*(XLE+./9.)))+2.*Z*SIGMA*(B*OM/CAPV)**2
7      *(.5*SIGMA*(CL+1.)*X3*(X16*X1+1.+C)+X112*X1*SIGMA*C*(XLE+.5)
8      +X112*X2*(XLE+.5)-SIGMA*X4*(.25*(CL+1.)*(XLE+.4)+X124*X1*
9      (XLE+X815))+.375*CLA*(XLE+./9.))-Z*X16*(XLE+XP15)*
$      (B*OM/CAPV)**4)
   B1A=2.*ZETAA*OM/OMEGNA+.125*BETA*CAPF*A*RHO*B/XIA*(CAPV/OMEGNA)**2
1      *(Z*(2.-XN)*SIGMA*VAR+X13*(2.-XN)*SIGMA**2*CAPA*Z*B*OM/CAPV)
2      +2.*RHO*B/XIA*(CAPV/OMEGNA)**2*Z*CAPA*SIGMA**2*CAPA*G/OM
3      *(SIGMA**2*X4*(CL+1.)*(.125*X1*(XLE+.4)+X23*(1.+C)*(XLE+.375))
4      +.5*X1*SIGMA**2*X4*(X124*X1*(XLE+X815)+X16*(1.+C)*(XLE+.5))
5      -.5*SIGMA*(CL+1.)*X3*(.5*X1*SIGMA*C+.5*X2+2.*SIGMA*C-.25*CLA)
6      +(B*OM/CAPV)**2*(X124*X1*(XLE+X815)+X16*(CL+1.)*X3
7      +X16*(1.+C)*(XLE+.5)))
   A1H=-(OM/OMEGNA)**2*XM*B**2*XALPHA/XIA+.125*BETA*CAPF*A*RHO*B/XIA
1      *(CAPV/OMEGNA)**2*((2.-XN)*SIGMA*VAR+2.*SIGMA**4*XM*BETA
2      *CAPA*SCRIPL/CAPH)+RHO/XIA*(CAPV/OMEGNA)**2*(CAPV/OM)**2*
3      SIGMA*CAPA*G*(2.*SIGMA**3*X4*(.5*(CL+1.)*X2*X3-.125*X1*CLH*X3)
4      -2.*Z*SIGMA*(B*OM/CAPV)**2*(SIGMA*X4*(X23*(CL+1.)*(XLE+.375)
5      +X112*X1*(XLE+.5))+.25*CLH*X3-.5*SIGMA*(CL+1.)*X3*(.5*X1+2.))
6      -Z*X13*(B*OM/CAPV)**4*(XLE+.5))
   B1H=.125*BETA*CAPF*A*RHO*B/XIA*(CAPV/OMEGNA)**2*
1      (Z*(2.-XN)*SIGMA*VAR+Z*(2.-XN)*SIGMA**2*CAPA*B*OM/CAPV)
2      +2.*RHO*B/XIA*(CAPV/OMEGNA)**2*CAPV*Z*SIGMA**2*CAPA*G/OM*
3      (SIGMA**2*(CL+1.)*X4*(X13*X1*(XLE+.375)+X3)
4      +X124*SIGMA**2*X1**2*(XLE+.5)*X4+.5*SIGMA*(CL+1.)*X3
5      *(X2+.5*CLH)+(B*OM/CAPV)**2*(X112*X1*(XLE+.5)+.5*(CL+1.)*X3))
   IF(WITCH1)30,40,30
30 ZERO1=A1A+XLE*A1H
   ZERO2=B1A+XLE*B1H
   GO TO 300
40 A2A=-XLE-(OM/OMEGNH)**2*(XALPHA+XLE)+RHO/XM*(CAPV/OMEGNH)**2
1      *(CAPV/(B*OM))**2*SIGMA*CAPA*G*(2.*SIGMA**3*X4*
2      ((CL+1.)*(X13*X1*SIGMA*C+X13*X2+SIGMA*C+.25*CLA)
3      +.5*X1*(X112*X1*SIGMA*C+X112*X2+.375*CLA))
4      -2.*Z*SIGMA*(B*OM/CAPV)**2*(SIGMA*X4*(.25*(CL+1.)+X124*X1)
5      -.375*CLA+.5*SIGMA*(CL+1.)*(X16*X1+1.+C)-X112*X1*SIGMA*C
6      -X112*X2)-Z*X16*(B*OM/CAPV)**4)
   B2A=-2.*ZETAH*OM*XLE/OMEGNH*2.+RHO/XM*(CAPV/OMEGNH)**2*CAPV/(B*OM)
1      *Z*SIGMA**2*CAPA*G*(SIGMA**2*(CL+1.)*X4*
2      (.125*X1*X23*(1.+C))+.5*SIGMA**2*X1*X4*(X124*X1+X16*(1.+C))
3      -.5*SIGMA*(CL+1.)*(.5*X1*SIGMA*C+.5*X2+2.*SIGMA*C-.25*CLA)
4      +(B*OM/CAPV)**2*(X124*X1+X16*(CL+1.)+X16*(1.+C)))
   ZERO1=A1A*A2H+B1H*B2A-B1A*B2H-A1H*A2A
   ZERO2=A1A*B2H+A2H*B1A-A1H*B2A-A2A*B1H
```

```
      ZERO2=ZERO2*5*CAPV/CM
300   RETURN
      END




      SUBROUTINE FRCFAC(CAPF,XN,RENO)
      IF(RENO-1828.57) 150,150,160
150   XN=1.0
      CAPF=64./RENO
      GO TO 190
160   IF(RENO-6644.7) 170,180,180
170   XN=0.0
      CAPF=.035
      GO TO 190
180   XN=.25
      CAPF=.316/RENO**XN
190   RETURN
      END
```

CHANNEL GEOMETRY

HEIGHT	WIDTH	ENTRANCE LOSS FACTOR	LENGTH UPSTREAM
0.100 IN	4.0625 IN	0.000	0.000 IN

PLATE PARAMETERS

THICKNESS	LENGTH	NO L.E. DISTANCE	SLOTWIDTH	NO E.A. DISTANCE
0.0625 IN	2.000 IN	-0.0625	0.03125 IN	0.1230

HOM. INTERTIA/UNIT WIDTH	ALPHA SPRING CONST	ALPHA NATURAL FREQ	ALPHA DAMPING RATIO
0.0362 LB-IN	669.75 IN-LB	68.01 RAD/SEC	0.00050

MASS/UNIT WIDTH	H SPRING CONST	H NATURAL FREQ	H DAMPING RATIO
0.1170 LB/IN	1390.6 LB/IN	54.51 RAD/SEC	0.00050

NATURAL FREQUENCIES

NO VIRTUAL AIRMASS	NO VIRTUAL AIRMASS	VIRTUAL AIRMASS	VIRTUAL AIRMASS
89.76 RAD/SEC	46.05 RAD/SEC	88.40 RAD/SEC	45.08 RAD/SEC
14.29 CYCLES/SEC	7.33 CYCLES/SEC	14.07 CYCLES/SEC	7.18 CYCLES/SEC

FLOW PARAMETERS

FLUID DENSITY	KINEMATIC VISCOSITY	CROSSFLOW LOSS COEF
4.34-005 LB/CU IN	2.34-002 SQ IN/SEC	0.600

RESULTS

  FLUID ACCELERATION CONSIDERED

    FLUTTER SPEED = 3.6243+001 IN/SEC

    FLUTTER FREQUENCY = 67.85 RAD/SEC = 10.80 CYCLES/SEC

    RATIO OF PITCHING AMPLITUDE TO DIMENSIONLESS TRANSLATION AMPLITUDE = 0.7344

    PHASE ANGLE BETWEEN PITCHING AND TRANSLATION = -1.2199 RAD = -69.894 DEG

  FLUID ACCELERATION NOT CONSIDERED

    NO SOLUTION FOUND BELOW SPEED = 2.5000+003 IN/SEC

SAMPLE PRINTOUT

REFERENCES

1. Spence, R. W.; and Durham, F. P.: The Los Alamos Nuclear Rocket Program. Astronautics and Aeronautics, Vol. 6, June 1965, pp. 42-46.

2. Miller, D. R.; and Kennison, R. G.: Theoretical Analysis of Flow-Induced Vibration of a Plate Suspended in a Flow Channel. Paper No. 66-WA/NE-1, ASME Winter Annual Meeting, 1966.

3. Burgreen, D.; Byrnes, J. J.; and Benforado, D. M.: Vibration of Rods Induced by Water in Parallel Flow. Trans. ASME, Vol. 80, 1958, pp. 991-1001.

4. Bland, S. R.; Rhyne, R. H.; and Pierce, H. B.: Study of Flow-Induced Vibrations of a Plate in Narrow Channels. Trans. ASME, J. Engineering for Industry, Vol. 89, Series B, Nov. 1967, pp. 824-830.

5. Woolston, D. S.; and Runyan, H. L.: Some Considerations on the Air Forces on a Wing Oscillating Between Two Walls for Subsonic Compressible Flow. J. Aeronautical Sciences, Vol. 22, Jan. 1965, pp. 41-50.

6. Toebes, G. H.; and Eagleson, P. S.: Hydroelastic Vibrations of Flat Plates Related to Trailing Edge Geometries. Trans. ASME, J. Basic Engineering, Vol. 81, Dec. 1961, pp. 671-678.

7. Marris, A. W.: A Review on Vortex Sheets, Periodic Wakes, and Induced Vibration Phenomena. Trans. ASME, J. Basic Engineering, Vol. 86, June 1964, pp. 185-196.

8. Thorpe, J. F.: A Parallel Duct Flow Problem. Ph.D. Thesis, Univ. of Pittsburgh, Pittsburgh, Pennsylvania, 1960.

9. Rouse, H.; and Howe, J. W.: Basic Mechanics of Fluids. John Wiley & Sons, 1953.

10. Kays, W. M.: Loss Coefficients for Abrupt Changes in Flow Cross Section with Low Reynolds Number Flow in Single and Multiple Tube Systems. Trans. ASME, Vol. 72, 1950, pp. 1067-1074.